Division of Molecular Structural Biology
Department of Medical Biochemistry and Biophysics
Karolinska Institutet, Stockholm, Sweden

CYSTEINE BIOSYNTHESIS IN MYCOBACTERIUM TUBERCULOSIS AS POTENTIAL DRUG TARGET

Katharina Brunner

Karolinska Institutet

Stockholm 2017

Published by Karolinska Institutet.
Printed by E-Print AB 2017

ISBN 978-91-7676-604-0

Institutionen för medicinsk biokemi och biofysik

Cysteine biosynthesis in Mycobacterium tuberculosis as potential drug target

THESIS FOR DOCTORAL DEGREE (Ph.D.)

AKADEMISK AVHANDLING

som för avläggande av medicine doktorsexamen vid Karolinska Institutet offentligen försvaras i Samuelssonsalen, Scheelelaboratoriet, Tomtebodavägen 6, Karolinska Institutet, Solna

Fredagen den 12 maj, 2017, kl 10:00

Av

Katharina Brunner

Principal Supervisor:
Prof. Gunter Schneider
Karolinska Institutet
Department of Medical Biochemistry and Biophysics
Division of Molecular Structural Biology

Co-supervisor:
Dr. Robert Schnell
Karolinska Institutet
Department of Medical Biochemistry and Biophysics
Division of Molecular Structural Biology

Opponent:
Prof.ssa Barbara Campanini
Università degli Studi di Parma
Dipartimento di Scienze degli Alimenti e del Farmaco

Examination Board:
Prof. Ralf Morgenstern
Karolinska Institutet
Institute for Environmental Medicine

Dr. Pål Stenmark
Stockholms Universitet
Department of Biochemistry and Biophysics

Dr. Ylva Ivarsson
Uppsala Universitet
Department of Chemistry

To

Gottfrank & Dorian Stain

ABSTRACT

The bacterium *Mycobacterium tuberculosis* is the underlying cause of tuberculosis, one of the most devastating infectious diseases, causing 1.4 million deaths in 2015. In addition one third of the global population is infected with latent tuberculosis, during which the bacilli remain viable in a dormant state, characterized by slow growth rates and changes in metabolism. It was shown that the underlying genes of sulfur assimilation and L-cysteine biosynthesis are essential for the survival of *Mtb* during dormancy. The availability of sulfur and the subsequently produced L-cysteine is directly linked to increased survival of *Mtb* inside host macrophages, because the first line of defense of *Mtb* against reactive oxygen and nitrogen species relies on mycothiol, the functional analog to glutathione in mycobacteria and the redox active sulfhydryl group of mycothiol is directly derived from L-cysteine. Hence the enzymes of the sulfur assimilation pathway and L-cysteine biosynthesis have been proposed as potential targets for novel antimycobacterial drugs.

Within the scope of this thesis, mycobacterial CysC, the APS kinase domain of the mycobacterial sulfur activation complex was mechanistically and structurally characterized. Phosphoryl group transfer from ATP to APS was shown to follow a conserved mechanism found in several species. In addition mutation of an L-cysteine residue in the lid region closing off the ATP binding site resulted in impaired ATP binding and prevented catalysis. The structural characterization included a comparison of mycobacterial CysC and the crystal structures to the two human homologs and it was found that the substrate binding sites for APS and ATP in the three enzymes shared a high degree of sequence identity, hence inhibitor development specifically targeting the mycobacterial enzyme was considered to be very challenging.

The three mycobacterial L-cysteine synthases, CysK1, CysK2 and CysM are upregulated during different metabolic states of *Mtb*. A high-throughput screening campaign of CysM identified a class of urea-based active site binders. Subsequent *in vitro* validation and organic synthesis of compounds to establish structure activity relationships in combination with structural based methods allowed the identification of seven potent CysM inhibitors. The affinities were found to be in the low micromolar range. The identified compounds did not only decrease CysM activity, but also showed bactericidal potency in a nutrient starvation model. CysK1 and CysK2 were also tested against a library of 71 compounds that were used for *in vitro* validation of CysM. In total four compounds were found to inhibit CysK1 and CysK2 and were also among the best inhibitors targeting CysM, suggesting that the identified inhibitors might provide a valuable starting point towards the development of a drug targeting all three L-cysteine synthases simultaneously.

LIST OF SCIENTIFIC PAPERS

I. Ömer Poyraz, **Katharina Brunner**, Bernhard Lohkamp, Hanna Axelsson, Lars GJ Hammarström, Robert Schnell, Gunter Schneider. (2015). ”Crystal Structures of the Kinase Domain of the Sulfate-Activating Complex in *Mycobacterium tuberculosis*” PLoS One **10**(3):e0121494.

II. **Katharina Brunner**, Selma Maric, Rudraraju Srilakshmi Reshma, Helena Almqvist, Brinton Seashore-Ludlow, Anna-Lena Gustavsson, Ömer Poyraz, Perumal Yogeeswari, Thomas Lundbäck, Michaela Vallin, Dharmarajan Sriram, Robert Schnell and Gunter Schneider. (2016). “Inhibitors of the Cysteine Synthase CysM with Antibacterial Potency against Dormant *Mycobacterium tuberculosis*.” Journal of Medicinal Chemistry **59**(14):6848–6859.

III. **Katharina Brunner**, Eva Maria Steiner, Rudraraju Srilakshmi Reshma, Dharmarajan Sriram, Robert Schnell and Gunter Schneider. “Profiling of *in vitro* Activities of Urea-based Inhibitors against Cysteine Synthases from *Mycobacterium tuberculosis*”. Manuscript.

CONTENTS

LIST OF ABBREVIATIONS

ADP	adenosine 5′-diphosphate
AMP	adenosine 5′-monophosphate
AMP-PNP	adenosine 5′-(β,γ-imido) triphosphate
APS	adenosine 5′-phosphosulfate
ATP	adenosine 5′-triphosphate
BCG	Bacille Calmette Guérin
CD	circular dichroism
DNA	deoxyribonucleic acid
DTT	dithiothreitol
ESI-MS	electrospray ionization mass spectrometry
FDA	Food and Drug Administration
HIV	human immunodeficiency virus
HTS	high-throughput screening
IFN	interferon
IL	interleukin
ITC	isothermal titration calorimetry
LAM	lipoarabinomannan
LHS	left-hand side
NADH	β-nicotinamide adenine dinucleotide
NADPH	β-nicotinamide adenine dinucleotide 2'-phosphate
NAS	*N*-acetyl serine
NMR	nuclear magnetic resonance
MDR	multidrug-resistant
MSH	mycothiol
MSSM	mycothiol disulfide
Mtb	*Mycobacterium tuberculosis*
NOD	nucleotide-binding oligomerization domain like receptor
OAS	*O*-acetyl-L-serine
OPS	*O*-phospho-L-serine
PAINS	pan assay interference compounds
PAMP	pathogen associated molecular patterns
PAPS	adenosine 3′-phosphate-5′-phosphosulfate
PAPSS	adenosine 3′-phosphate-5′-phosphosulfate synthetase
PIM	phosphatidylinositol mannan
PLP	pyridoxal 5′-phosphate
PP_i	pyrophosphate
RHS	right-hand side
RNS	reactive nitrogen species
ROS	reactive oxygen species
SAM	*S*-5′-adenosyl-L-methionine
SAR	structure-activity relationship
SL	sulfolipid
TDM	trehalose dimycolate
TLR	toll-like receptor
TNF	tumor necrosis factor
WHO	World Health Organization
XDR	extensively drug-resistant

1 MYCOBACTERIUM TUBERCULOSIS

1.1 THE HISTORY OF TUBERCULOSIS

Mycobacterium tuberculosis (*Mtb*) and humans share a common history for at least 70,000 years. The spread of the disease was accompanied by the migration of early humans out of Africa, as shown by population genomics studies (Comas, Coscolla et al. 2013). The first physical evidence of tuberculosis infection was found in human skeletons from the Neolithic era excavated in Israel and Syria showing typical bone lesions for spinal tuberculosis, underpinned by the presence of mycolic acids and ancient mycobacterial DNA extracted from bones (Baker, Lee et al. 2015; Spigelman, Donoghue et al.). During the Neolithic era the increase of human population and density explain the successful spread of *Mtb* (Comas, Coscolla et al. 2013), rather than transmission from domesticated animals as proposed earlier (Diamond 1999).

Tuberculosis, also known as consumption or the white plague had its peak between the 17th and 19th century. At this time every fourth adult in Europe died from tuberculosis (Wilson 2004). It took until 1882 to understand the underlying cause of tuberculosis (Koch 1882). Robert Koch was the first to show that tuberculosis was an infectious disease caused by the bacterium *Mycobacterium tuberculosis* by performing animal experiments on guinea pigs and was subsequently awarded the Nobel Prize in Physiology and Medicine in 1905 (Cambau & Drancourt 2014).

In 1921, the bacille Calmette-Guérin (BCG) vaccine was developed, which is still the sole effective and licensed vaccine against tuberculosis today (Calmette 1922; Hatherill, Tait et al. 2016). Calmette and Guérin were sub-culturing virulent *Mycobacterium bovis* isolates for thirteen years before the strain showed sufficient attenuation to be safe enough to be used in humans (Luca & Mihaescu 2013). In 1943, the first antimycobacterial drug, the antibiotic streptomycin became available. This, in combination with the BCG vaccine, resulted in mortality rates starting to drop and, hope to fully eradicate tuberculosis emerged. Funding and interest in tuberculosis research declined until (Keshavjee & Farmer 2012) co-infections of HIV and tuberculosis and infections with multidrug-resistant *Mtb* (MDR) were observed in the early 1990s and death tolls started to rise again (Comas & Gagneux 2009). In 1998 the first genome of *Mtb* was sequenced (Cole, Brosch et al. 1998). To date there are seven known *Mtb* strain lineages that affect humans. The *Mtb* lineages are associated with different geographical regions and all evolved from one common ancestral strain. Whole genome sequencing revealed that the different *Mtb* lineages are genetically much more diverse than expected, and this diversity can be linked to human migration events (Hershberg, Lipatov et al. 2008). One example is the successful spread of the Beijing lineage from East Asia towards Europe along the Silk Road (Merker, Blin et al. 2015). Tuberculosis infections caused by the Beijing lineage had high prevalence in Asia and the former Soviet Union in the past. To date, this lineage has spread over the entire world and more recent tuberculosis outbreaks caused by the Beijing lineage are associated with drug resistance (Rufai, Sankar et al. 2016).

In 2015 about two million people died from tuberculosis worldwide and additional 10.4 million newly infected were counted globally. On top of that, one third of the global population carries an asymptomatic latent tuberculosis infection that is reactivated in

approximately ten percent of all cases and MDR *Mtb* is on the rise. The observation that currently used antibiotics are ineffective in treating latent tuberculosis infections or MDR-infections indicates that novel antimycobacterial drugs are urgently needed to achieve the goal of the WHO to eradicate tuberculosis by 2035 (World Health Organization 2016).

1.2 PATHOGENESIS OF TUBERCULOSIS INFECTION

After initial contact between host and *Mtb*, the infection can either be cleared, controlled by the immune system or progress into active tuberculosis (Salgame, Geadas et al. 2015). The active form of tuberculosis, known as pulmonary tuberculosis, mostly affects the lungs and is initiated by a characteristic lung inflammation (Hopewell, Kato-Maeda et al. 2016). If tuberculosis remains untreated, it eventually results in death (Fitzgerald, Sterling et al. 2015). Individuals carrying active tuberculosis can easily spread the infection by expelling *Mtb*-containing air droplets, produced through coughing and sneezing (**Fig. 1**). Symptoms of active tuberculosis include fever, coughing, with occasional blood in the sputum, weight loss, night sweats and changes in the opacity of certain areas in chest radiographs (Fitzgerald, Sterling et al. 2015).

Specific human sub-populations show an increased risk of developing tuberculosis. Amongst those are individuals living in developing countries, suffering from malnutrition, who are co-infected with HIV, or health care workers, facing higher exposure to infectious individuals. In addition, young adults in their early twenties, smokers and patients treated with immune suppressants are part of this group. Interestingly gender also plays a role, as men are more prone to acquire infection (World Health Organization 2016) (Fogel 2015).

Latent tuberculosis is defined as measurable specific immune response against *Mtb* in the absence of active tuberculosis symptoms and is considered to be controlled by the host immune system (Gengenbacher & Kaufmann 2012) and individuals carrying a latent tuberculosis infection are not contagious (Ernst 2012). Two billion people, which account for one third of the world population, are carrying such a latent tuberculosis infection, which represents a huge infectious cohort, because ten percent of latent tuberculosis infections are reactivated. The reasons for reactivation of latent tuberculosis are poorly understood, but rely on the complex cross-talk between the pathogen and the host immune system (Philips & Ernst 2012; Vynnycky & Fine 2000; World Health Organization 2016).

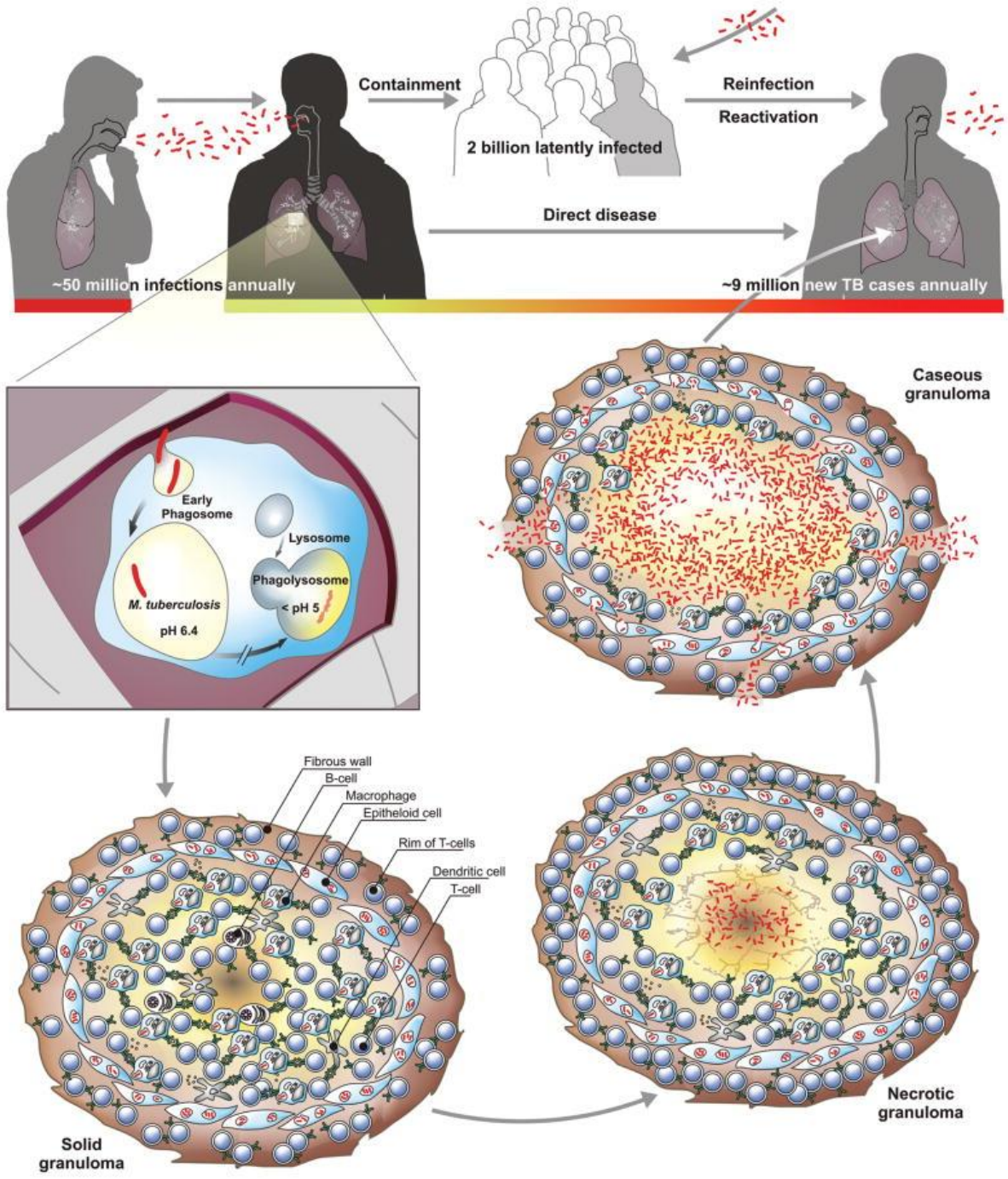

Figure 1. The upper panel shows the route of tuberculosis transmission between infected individuals and transformation into latent tuberculosis. The lower panel illustrates the progress of *Mtb* infection from phagocytosis through granuloma formation and necrosis. After phagocytosis *Mtb* survives inside the host macrophages by interfering with phagolysosomal fusion and induces formation of a solid granuloma. The granuloma matures via the necrotic phase to a caseous granuloma, lower panel. Reprinted by permission from Oxford University Press: FEMS Microbiology Reviews (Gengenbacher & Kaufmann 2012), copyright 2012.

1.2.1 Immune response against invading bacteria

The innate immune response plays a crucial role in the clearance of invading bacteria. Upon bacterial infection immune cells, such as macrophages and neutrophils, recognize a broad spectrum of microbes via pathogen recognition receptors on their surface, and induce phagocytosis, which subsequently leads to antigen processing and the involvement of other immune cells via cell-cell communication (Martin, Carey et al. 2016). During phagosome maturation the bacteria are exposed to low pH, reactive oxygen (ROS) and reactive nitrogen species (RNS) and cationic antimicrobial peptides, leading to membrane disorganization, and the degradation of bacterial lipids and proteins (Gengenbacher & Kaufmann 2012). Eventually the phagosome fuses with the lysosome in which the invading bacterium is digested and components specific for pathogens, also known as pathogen associated molecular patterns (PAMPs), are displayed. These PAMPs further activate distinct pattern recognition receptors, such as NODs and TLRs, residing in different cell compartments, and induction of the adaptive immune response is initiated in addition to the innate immune response (Awuh and Flo 2016; Akira, Uematsu et al. 2006). To control the mycobacterial infection, macrophages need to be fully activated, which requires the presence of T-cells, such as CD4+, CD8+, Th17 and regulatory T-cells. Particularly important is the Th1 dominant response, which leads to secretion of IL-12 and TNF-α and additional pro-inflammatory cytokines that lead to inflammatory signaling and induction of antimicrobial pathways. Usually the intruding microbe is cleared before any sign of disease or symptoms are observed (Weiss & Schaible 2015; Awuh & Flo 2016; Martin, Carey et al. 2016).

1.2.2 Influence of macrophage phenotype on progression of tuberculosis

Upon encountering an invading bacterium, the basal macrophage phenotype is skewed towards the classical activation phenotype, which contributes in a Th1 dominant immune response upregulating antimicrobial pathways. The classical activation subsequently leads to necrosis and is considered to be host-protective in early tuberculosis infection (Martin, Carey et al. 2016). A different macrophage phenotype is evoked upon alternative activation (Martinez & Gordon 2014). The immune response of this macrophage phenotype is weakly antibacterial and leads to wound healing and damage resolution and is considered as host-protective during later stages of infection to prevent tissue damage (Mosser & Edwards 2008).

However, after *Mtb* enters the human host via the alveoli of the lungs, *Mtb* faces alveolar macrophages first, which comprise a mixed phenotype and play a role in surveillance and destruction of invading bacteria. Immediate full activation of alveolar macrophages would lead to rapid destruction of lung tissue therefore the triggered immune response is dampened, and in turn allows *Mtb* to successfully enter the host and establish their niche inside the macrophages of the human lungs (Hussell & Bell 2014).

1.2.3 Granuloma formation – a hallmark of tuberculosis

Granulomas are the classical histological lesions developing during pathogenesis of tuberculosis and in the initial stage they are defined as an aggregate of macrophages (Philips & Ernst 2012; Martin, Carey et al. 2016). In later stages also other immune cells, such as dendritic cells, neutrophils, T-cells and B-cells join the this formation (**Fig. 1**) (Philips &

Ernst 2012). Initially it was assumed that granulomas are host-protective, by walling-off mycobacteria and keeping them from disseminating. Whereas this might be true in the later stage of infection in which granulomas become fibrotic and calcify, it is rather the opposite during early infection, in which they act as infection promotor. Close proximity of the cells in the granuloma facilitate cell-to-cell spread and expansion of the mycobacterial population. For initiation of granuloma formation one infected alveolar macrophage is sufficient (Davis & Ramakrishnan 2008). In this stage the infected macrophage recruits other macrophages which subsequently differentiate. Mycobacterial ketomycolic acids direct the differentiation towards the foamy type of macrophages which are associated with necrotic tissue (Peyron, Vaubourgeix et al. 2008). Characteristic for the foamy type is a high amount of lipids, for example cholesterol that is imported in order to serve as a carbon source during chronic infection (Pandey & Sassetti 2008). The mycobacterial cell wall components phosphatidylinositol mannan (PIM), lipoarabinomannan (LAM) and trehalose dimycolate (TDM) cause formation of multinucleated giant cells (Puissegur, Lay et al. 2007). Infected dendritic cells allow migration of *Mtb* from the lungs to lymph nodes to present antigens to naïve T-cells (Lay, Poquet et al. 2007). T-cells can either be diffusely spread in between the other cells of the granuloma or form an outer layer around the aggregate structure and are responsible in maintaining organized granulomas and control *Mtb* progression after the active phase of tuberculosis. Granulomas were shown to be highly dynamic structures in which cells can freely diffuse in and out (**Fig. 1**) (Philips & Ernst 2012). The center of a granuloma is usually called caseum and comprises a cheese-like consistency resulting from coagulative tissue necrosis. If the host is capable of controlling *Mtb*, then necrosis is stalled and the caseum is eventually replaced by calcified and fibrotic tissue and infection is considered to be latent. However if tuberculosis progresses, the caseum is expanded leading to necrosis and cavity formation in the lungs. The breakdown of the surrounding lung tissue allows spreading of *Mtb* into the nearby airways and facilitates dissemination and transmission, referred to as active tuberculosis (Martin, Carey et al. 2016).

1.2.4 Active and latent tuberculosis

The sharp discrimination between active tuberculosis and latent tuberculosis infection is heavily disputed and considered as outdated, because it draws the picture of an oversimplified, two-state binary model of disease that opposes the knowledge we gained about tuberculosis (Salgame, Geadas et al. 2015; Martin, Carey et al. 2016; Mack, Migliori et al. 2009; Horsburgh, Barry et al. 2015). For example, inside the lungs of patients carrying either variant of tuberculosis, both caseous and calcified granulomas have been observed in parallel (Lenaerts, Barry et al. 2015). Furthermore, *Mtb* itself is considered to be present in different metabolic states during active and latent tuberculosis. Gengenbacher and Kaufmann proposed a dynamic model of the two disease states, in which latent tuberculosis is characterized by a majority of dormant bacilli and a minority of some actively dividing *Mtb* that sense the environment in terms of nutrient availability and presence of oxygen. Inside the calcified granulomas the environment prohibits the presence of a large number of actively dividing *Mtb* and the majority remains dormant. If the granuloma transists into the caseous state, the bacilli awake from dormancy. Some remain in their dormant state though and still comprise the phenotypic inherent antimycobacterial drug resistance, which explains the

required long lasting tuberculosis treatment of at least six months (Gengenbacher & Kaufmann 2012).

1.2.5 *Mtb* interferes with the immune response of the host

Mtb has evolved to survive the host immune response, due to their long common evolutionary history. The bacterium interferes with well-established immune cell functions and survives inside host phagocytes including macrophages (Armstrong & Hart 1971). Degradation and processing of invading bacteria require fusion of the phagosome and the lysosome, which is achieved by a well order mechanism of interactions between phagosomal membrane proteins and phospholipids. Part of this mechanism is the recruitment of the GTPase, Rab7 to the phagosomal membrane and subsequent phosphorylation of phosphatidylinositol. *Mtb* however abolishes both steps and thereby evades digestion by macrophages (Philips & Ernst 2012). In addition *Mtb* interferes with proper functioning of the autophagy system that impedes intracellular growth of mycobacteria after it has been stimulated by IFNγ. Through disruption of membranes with the help of several type VII secretion systems, *Mtb* can escape into the cytoplasm, avoid necrosis and even infect adjacent cells (Hopewell, Kato-Maeda et al. 2016). Phagosome permeabilization triggers the release of IFNα and -β that in turn suppress expression of IL-1β, essential for controlling the *Mtb* infection (Mayer-Barber, Andrade et al. 2011; Novikov, Cardone et al. 2011). The mycobacterial cell wall contains various lipids that do not only protect *Mtb* from polar molecules and serve as a waxy barrier preventing antimycobacterial drugs to enter the cytoplasm, but they are also involved in direct interaction with the host. PIM and LAM stimulate innate immune and inflammatory response and serve as toll like receptor 2 agonists and LAM alters phagosome maturation. TDM, also known as mycobacterial cord-factor is recognized by two lectin receptors in macrophages and dendritic cells and transduces pro-inflammatory signals (Hopewell, Kato-Maeda et al. 2016). TDM alone is also sufficient to induce transient granuloma formation in mice (Copenhaver, Sepulveda et al. 2004).

1.2.6 Adaptation of *Mtb* to the harsh environment inside macrophages

Upon phagocytosis *Mtb* has to withstand drastic environmental changes, characterized by low pH, nutrient starvation, lack of oxygen and presence of ROS and RNS (Gengenbacher & Kaufmann 2012; Martin, Carey et al. 2016). In response to these challenges the mycobacterial metabolism changes completely. *Mtb* switches from an actively dividing state to a non-replicating persistent state during which also the susceptibility to antimycobacterial drugs is decreased, known as phenotypic drug resistance, a form of resistance conferred by a metabolic state that is not encoded in the genome. During the non-replicating state, which is also termed dormancy, the bacilli remain fully viable but at a very low metabolic rate (Gengenbacher & Kaufmann 2012).

Mtb is capable of withstanding low pH within the phagolysosome (Schaible, Sturgill-Koszycki et al. 1998), which is to some degree caused by the unique composition of the mycobacterial cell wall. The absence of full acidification of the phagolysosome in macrophages however is attributed to inhibition of the phagosomal ATPase by *Mtb* and the presence of a urease that cleaves urea. The buffering property of the produced ammonia stabilizes the pH at a slightly higher level than usual (Gengenbacher & Kaufmann 2012).

While engulfed inside the macrophage, *Mtb* scavenges nutrients from the host environment (Niederweis 2008; Martin, Carey et al. 2016). Upon switching from carbohydrates as a carbon source to lipids from foamy giant cells, the acetyl moiety of acetyl-CoA is replaced by propionyl and leads to toxic by-products for *Mtb* (Gengenbacher & Kaufmann 2012). In order to avoid harming itself, the bacterium uses propionyl-CoA to produce PDIM, which are considered a virulence factor (Lee, VanderVen et al. 2013). In good agreement with this is the observation that genes involved in fatty acid biosynthesis are upregulated (Schnappinger, Ehrt et al. 2003).

Inside caseous and calcified granulomas *Mtb* faces hypoxia (Via, Lin et al. 2008). To counterstrike hypoxia a complex transcriptional network including the DosR regulon is upregulated and genes are transcribed to stabilize proteins, avoid DNA damage, switch on alternative electron transport chains and induce angiogenesis inside the granulomas to increase oxygen content (Leistikow, Morton et al. 2010; Martin, Carey et al. 2016).

Inside the macrophages *Mtb* also faces damage of DNA, cell wall and proteins by ROS and RNS. The phagocytosed bacteria usually are killed by these radicals that primarily target Fe-S clusters and sulfhydryl groups in proteins and nucleotide bases in nucleic acids (Martin, Carey et al. 2016). ROS and RNS induce transcription of the DosR regulon also and additional detoxifying enzymes are expressed in *Mtb* (Kumar, Toledo et al. 2007). Reactive nitrogen species are not only produced by macrophages, but also by *Mtb* itself, and are considered to act bacteriostatic rather than bactericidal (Cunningham-Bussel, Zhang et al. 2013). The detoxifying enzyme superoxide dismutase disarms superoxide radicals and is part of a macromolecular oxidoreductase complex that copes with oxidative stress and maintains the cytosolic redox homeostasis in *Mtb*. To cope with hydrogen peroxide, *Mtb* uses catalase-peroxidase (Nambi, Long et al. 2015; Martin, Carey et al. 2016). NADH-dependent peroxidase and peroxynitrite reductase is another complex involved in detoxification of ROS and RNS, consisting of an alkyl hydroperoxide reductase, an oxidoreductase, a dihydrolipoamide acyltransferase and lipoamide dehydrogenase (Ehrt & Schnappinger 2009).

1.3 MAINTENANCE OF REDOX HOMEOSTASIS IN *MTB*

To maintain intracellular redox homeostasis during the exposure to oxidative stress, *Mtb* produces mycothiol (MSH) which is the functional analog of glutathione in *Mtb* and related genera (**Fig. 2A**) (Bornemann, Jardine et al. 1997). MSH is the major low-molecular-weight thiol produced in *Mtb* and present in millimolar concentration inside the mycobacterial cell (Bhave, Muse et al. 2007). MSH biosynthesis involves five enzyme-catalyzed reactions. The fourth step of MSH biosynthesis directly links maintenance of redox homeostasis to the availability of L-cysteine and emphasizes the importance of L-cysteine biosynthesis also during the dormant state of *Mtb*, while engulfed inside the macrophage. MSH maintains the reducing intracellular environment and thereby acts as a thiol redox buffer (Jothivasan & Hamilton 2008; Fan, Vetting et al. 2009). Toxic oxidants, which are produced inside macrophages to combat *Mtb*, are reduced by MSH, which in turn is oxidized to MSSM. In order to maintain high concentrations of MSH, the NADPH-dependent flavoprotein mycothiol disulfide reductase constantly reduces MSSM to MSH (**Fig 2B**). Mutants deficient in MSH biosynthesis have been shown to be more sensitive to oxidative stress, confirming the importance of this system in tuberculosis pathogenesis (Jothivasan & Hamilton 2008).

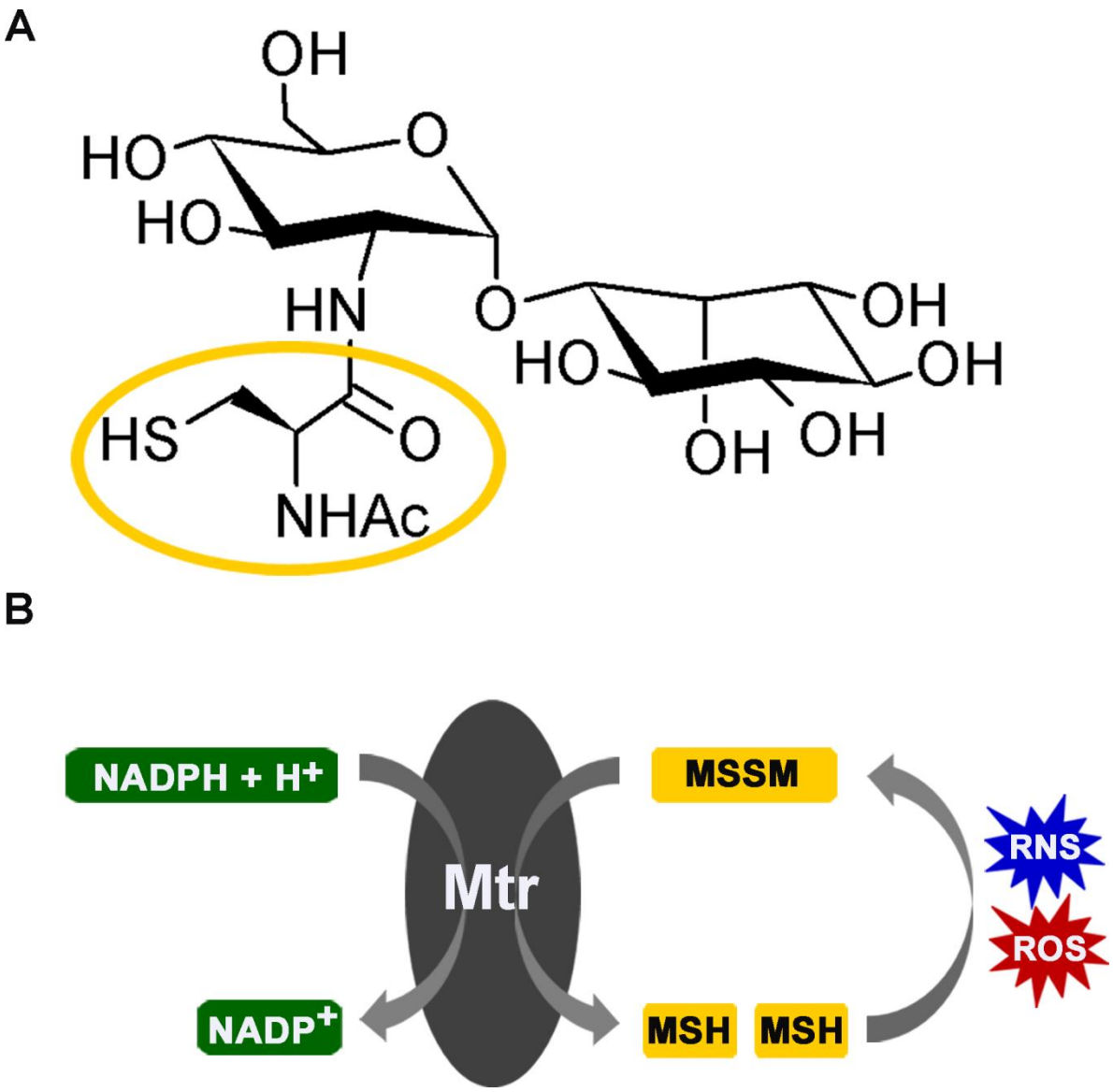

Figure 2. A) Chemical structure of mycothiol (MSH), the dominant low-molecular-weight thiol in mycobacteria. The L-cysteine derived redox-active part is encircled in yellow. **B)** RNS and ROS oxidize MSH to MSSM which is regenerated by the NADPH-dependent flavoprotein mycothiol disulfide reductase to maintain a high intracellular level of MSH.

1.4 TUBERCULOSIS TREATMENT AND CHALLENGES

The current recommendation to treat new cases of pulmonary tuberculosis is a daily regimen of multiple antibiotics for at least six months and is considered standard treatment for presumable drug-susceptible *Mtb* (World Health Organization 2016). The initial induction phase takes two months and includes treatment with isoniazid, rifampicin and pyrazinamide. In addition, ethambutol or streptomycin is administered to circumvent unrecognized drug resistance against any of the three core drugs. Ethambutol is avoided in young children, if possible, because toxic adverse drug effects are difficult to detect in this patient group. As soon as drug-susceptibility to the three core drugs of the regimen is confirmed, the fourth antimycobacterial drug is discontinued. The induction phase is followed by a consolidation

phase, in which treatment with isoniazid and rifampicin is continued for at least four months (Horsburgh, Barry et al. 2015).

Treatment of tuberculosis takes much longer compared to treatment of any other bacterial infection. This is attributed to the high rate of spontaneous mutations in the genome of *Mtb* and the subsequent development of drug resistance (Fogel 2015). In particular the Beijing lineage of *Mtb* and strain *W* and related *W*-like families are associated with a high occurrence of drug resistance (Kremer, Glynn et al. 2004). Although much effort is put in identifying the underlying genetic differences between lineages, no genetic advantages have been identified that entails a higher occurrence of drug resistance in this particular lineage (Lawn & Zumla 2011). In general *Mtb* does not appear to gain mutations associated with drug resistance via transposition or horizontal gene transfer (Smith, Wolff et al. 2013). However previous treatment with antimycobacterial drugs, incomplete treatment, not complying with treatment recommendations or inadequate treatment regimens can increase the mutation rate and leading to faster emerge of drug resistances (Fogel 2015). In addition to spontaneous mutations resulting in drug resistance, also drug-susceptibility towards certain antimycobacterial drugs varies, dependent on the metabolic state of *Mtb* itself. Current treatments target non-replicating *Mtb* only to a small extent and leave two billion people untreated (Wallis, Maeurer et al. 2016).

Although the overall numbers of tuberculosis deaths have been decreasing over the past years, an increase of drug resistance incidences has been observed over the past thirty years, which emphasizes the urge to develop new drugs targeting *Mtb* (Lawn & Zumla 2011). In the year 2015, 480,000 new cases of MDR *Mtb* have been reported, among which ten percent account for extensively drug-resistant (XDR) *Mtb*. MDR strains are resistant against at least isoniazid and rifampicin, whereas XDR strains are in addition resistant to fluoroquinolone and one of the three injectable antibiotics, capreomycin, kanamycin or amikacin. In addition to MDR *Mtb*, cases of totally drug resistant *Mtb*, characterized by resistance against all currently used antimycobacterial drugs have been reported (World Health Organization 2016).

The highest numbers of XDR incidences have been counted in India, China and the Russian Federation and together they account for a total of 45% of all MDR tuberculosis cases (World Health Organization 2016). The WHO recommends drug-susceptibility testing for all treated patients however infrastructures for culturing *Mtb* are not always available, especially not in areas with very high incidence rates, which often appear to be in developing countries. These patients often undergo blind therapy in combination with intermittent treatment leading to increased rates of drug resistance. Treatment of MDR *Mtb*, especially, is very costly and long lasting and also shows higher rates of toxic adverse effects, resulting in drug-induced irreversible destruction of the lung tissue, associated with impaired organ functionality (Lawn & Zumla 2011).

1.5 EARLY STAGE DRUG DISCOVERY

The development of a novel drug is a very time consuming and costly process. It is estimated that the entire process from discovery to approval of a drug takes approximately fifteen years with associated costs of one billion dollar. Drug discovery is the first stage of the drug development process that in the best case results in the approval of a candidate drug. One method to discover a new drug is the target-based approach, which is initiated by the choice of a target that requires extensive characterization and evaluation of disease association. This step, also known as target validation, employs laboratory techniques that are required for *in vitro* and *in vivo* validation, such as expression profiling, biochemical assays, whole cell and animal models. Target validation is followed by hit identification, which is often achieved by high-through put screening. The through-put can vary, dependent on the choice of screening method. In the target-based approach an already established biochemical or activity assay that proofs interaction with or inhibition of the target of choice is optimized to fit the purpose of high-throughput liquid handling and is used for screening of compound libraries against the target of interest (Hughes, Rees et al. 2011). The compound libraries are composed of chemicals with drug-like properties which usually obey Lipinski's rule of five, which states that a drug which is orally active does not comprise more than five hydrogen bond donors and not more than ten hydrogen bond acceptors. Furthermore, the molecular mass does not exceed 500 Da and the ClogP is not higher than 5 (Lipinski, Lombardo et al. 2001; Hughes, Rees et al. 2011). The screening campaign for CysM (paper II) was performed in a target-based fashion. **Fig. 3** shows the different stages of the drug development process and also shows which stages of the drug development process were covered during inhibitor development targeting CysM, which will be discussed later in chapter 3.2. The advantages of target-based screens are a much higher throughput, reduced variability in biological samples and the rapid assessment of the effect on the target. Disadvantages of target-based approaches are the difficulty to select disease-relevant targets and that the observed direct effects on the target cannot be translated to *in vivo* activities, due to redundancy of pathways or drug permeability issues (Zuniga, Early et al. 2015; Hughes, Rees et al. 2011; Chai & Mátyus 2015).

Alternatively, a phenotypic whole cell assay can be performed, in which the compound is added to live cells and the effect of the added compound is validated based on the phenotypic changes after treatment. In this approach, the target is not necessarily validated or not even known. Target identification, characterization and validation are performed in subsequent steps. The major advantage of phenotypic-based approaches is the direct observation of *in vivo* activity. Disadvantages are a much lower through put, the unknown targets and the associated effort to understand the mode of action (Chai & Mátyus 2015; Hughes, Rees et al. 2011; Zuniga, Early et al. 2015). Phenotypic approaches are more successful, in the discovery of novel first-in-class drugs compared to target-based approaches, which switches when follow up drugs are discovered (Swinney & Anthony 2011).

The next stage is the hit refinement process, in which the hits obtained are compared and further characterized to demonstrate dose-dependency and generate dose-response curves with orthogonal assays. The hits are ranked according to their potency and clustered into groups based on their chemical properties. During this stage also initial structure-activity relationships are established, which may include reiterative synthesis of compounds that are

not available in the compound library, to determine the common scaffold of hit series. In the hit to lead stage the identified hit series are evaluated in an *in vivo* model with the aim to increase potency and selectivity of the hits, but also with regard to their pharmacokinetic and toxicological properties. Structure-activity relationships are established in a systematic way to assign the functional groups of a hit with increased potency and/or selectivity. In this stage also structure based drug design, such as X-ray crystallography and NMR are employed. Crucial at this point is the assessment of the potential of a compound becoming a drug, which is indicated by solubility and permeability of the compound. The final stage of the drug discovery process is the lead optimization stage, during which suboptimal properties of the lead compounds are improved, while the desired properties are maintained (Hughes, Rees et al. 2011). The number of compounds decreases tremendously during the drug discovery process and often not a single compound makes the transition into a clinical candidate that enters the drug development stage, including clinical trials (Bleicher, Bohm et al. 2003).

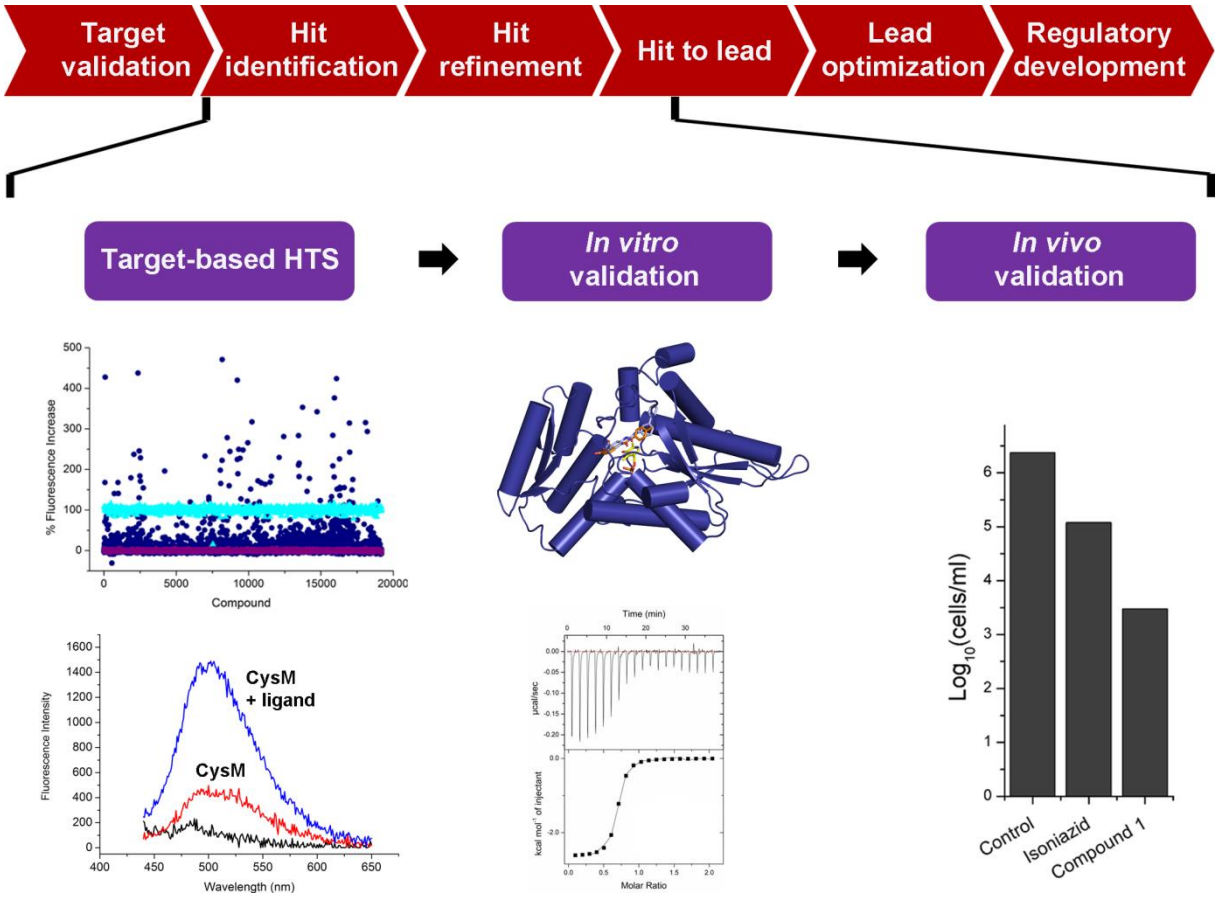

Figure 3. Flow scheme of the different stages of the drug development process (red), with focus on early stage drug discovery (purple). The lower panel of the figure summarizes the major steps towards development of inhibitors targeting CysM (paper II), including high-throughput screening, *in vitro* and *in vivo* validation. Scatterplot from the target-based HTS, which was based on the PLP fluorescence signal and the emission spectrum of the ligand free (red) and ligand bound (blue) enzyme are shown in comparison to the background (black). The *in vitro* target specific interaction is illustrated by the binding curve of the top inhibitor from an ITC experiment, and the crystal structures of target ligand complexes. *In vivo* validation of the antibacterial activity is illustrated by the antibacterial killing effect of the top CysM inhibitor in comparison to isoniazid.

Drug discovery of novel antimycobacterial drugs faces several organism specific challenges. One example is the slow growth rate that slows down the evaluation of all live-bacteria based tests. In order to perform research on *Mtb*, a laboratory of biosafety level 3 is required, which results in very costly facilities needed for the drug discovery process. The waxy cell wall containing many different lipids acts as a natural diffusion barrier that prevents penetration of drugs through the bacterial cell wall. The presence of efflux pumps that actively transport certain types of molecules out of the mycobacterial cell are in particular hard to tackle. Another obstacle is the presence of various microenvironments in which *Mtb* can survive and the simultaneous existence of several metabolic states of *Mtb.* (Zuniga, Early et al. 2015). Several animal models are used to study latent tuberculosis, however these models do not truly mimic infection in humans. One example is the mouse model, although frequently used immune response towards *Mtb* is different because granulomas do not progress into the caseous or calcified type. The bacterial burden can also differ a lot between mice and humans. Zebrafish are also often used as model organisms as they show caseation of granulomas however *Mycobacterium marinum* establishes the infection instead of *Mtb*. *In vitro* models such as the Wayne hypoxia model suffer from the absence of standardization, because different protocols exist and this model does not address adaptation of *Mtb* to other stress inducers (Alnimr 2015).

Even though mentioned challenges exist in the development of novel antimycobacterial drugs, several advances in drug development have been made in recent years. One example is bedaquiline, which was FDA-approved in 2012 for treatment of adults suffering from MDR pulmonary tuberculosis, where no alternative treatments are available (Cox & Laessig 2014). Bedaquiline was discovered by applying a phenotypic whole cell screen, using *Mycobacterium smegmatis* as a surrogate strain. The target was identified by isolating resistant mutants, followed by whole genome sequencing (Andries, Verhasselt et al. 2005). This approach has the advantage that it not only identifies the target, but also identifies mechanisms responsible for resistance or activation of the drug. Bedaquiline was shown to inhibit a mycobacterial ATP synthase found in the mycobacterial cell membrane and thereby preventing energy production of *Mtb* (Mikušová & Ekins 2017). During clinical trials of bedaquiline a mortality imbalance between the treated and placebo group was observed, however a direct link between bedaquiline and mortality of the patients could not be established (Cox & Laessig 2014; Diacon, Pym et al. 2014). Bedaquiline is one of four novel compounds that are currently in the advanced stages of clinical development. In addition to these four novel compounds, the three drugs, rifampicin, rifapentine and linezolid, which are already approved for treatment of tuberculosis, are currently undergoing further clinical trials. Rifampicin and rifapentine are tested if high doses are feasible for treatment at all and linezolid is tested in new drug regimens with already used antimycobacterial drugs (World Health Organization 2016; Wallis, Maeurer et al. 2016). Very recently, the drug-like molecule spiroisoxazoline SMARt-420 was shown to fully reverse resistance against ethionamide in *Mtb*, a prodrug that requires activation by mycobacterial enzymes. SMARt-420 activates an alternative bioactivation pathway for ethionamide that increased sensitivity towards the drug. Although SMARt-420 is still in its discovery stage, it opens interesting possibilities, for example temporary treatment with SMARts, to destroy resistant *Mtb* subpopulations during ordinary treatment, as proposed by the authors of this study (Blondiaux, Moune et al. 2017).

1.6 L-CYSTEINE BIOSYNTHESIS AS DRUG TARGET

The availability of L-cysteine has been shown to be of high importance for *Mtb* during infection. Up-regulation of underlying genes of L-cysteine biosynthesis under conditions reflecting dormancy revealed a link between L-cysteine necessity and latent tuberculosis (Voskuil, Visconti et al. 2004; Schnappinger, Ehrt et al. 2003). The genes significantly up-regulated included *cysD*, *cysNC* and *sirA*, which encode for enzymes important for sulfur assimilation and *cysM* and *cysK2*, genes encoding for two of the three mycobacterial L-cysteine synthases (Voskuil, Visconti et al. 2004; Voskuil, Bartek et al. 2011; Schnappinger, Ehrt et al. 2003; Betts, Lukey et al. 2002; Hampshire, Soneji et al. 2004). In addition, the redox-active moiety of mycothiol is a sulfhydryl group that is derived from L-cysteine and directly linked to mycobacterial redox defense against RNS and ROS inside macrophages (Bhave, Muse et al. 2007). Randomized transposon mutagenesis showed that mutants deficient in producing CysD, CysH, CysE, CysNC, CysO and CysM were severely attenuated in a macrophage and mouse model of dormancy (Rengarajan, Bloom et al. 2005). Inhibitors targeting mycobacterial CysH, the APS reductase providing sulfite for subsequent L-cysteine formation, have been successfully identified by a target-based screening approach. The strongest inhibitors were based on a 6H-pyrido[4,3-b]carbazole scaffold. These compounds reduced cellular levels of sulfur containing metabolites, such as sulfite, L-cysteine and mycothiol *in vivo* and showed bactericidal activity against dormant *Mtb* (Palde, Bhaskar et al. 2016). Hence targeting L-cysteine biosynthesis and the preceding sulfur assimilation pathway might be a valuable route for the discovery of novel antimycobacterial drugs. The mycobacterial L-cysteine biosynthesis is of particular interest, because of the complete absence of this pathway in humans (Schnell, Sriram et al. 2015).

1.7 SULFUR ASSIMILATION IN *MTB*

The first step in sulfur assimilation in *Mtb* (**Fig. 4**) is transport of inorganic sulfate by the CysT●W●A●SubI ABC transporter complex through the cytoplasmic membrane into the mycobacterial cytoplasm from the environment. The sulfate transporter consists of the two membrane spanning subunits CysW and CysT. The sulfate binding subunit, SubI, is connected via a lipid tail to the cytoplasmic membrane. On the cytoplasmic site, CysW and CysT each bind one copy of the nucleotide binding protein CysA (Wooff, Michell et al. 2002). Sulfate is thought to follow a similar transport route to that of phosphate, which first is imported via porins and subsequently transported through the cytoplasmic membrane by a specific phosphate transporter (Wolschendorf, Mahfoud et al. 2007; Rengarajan, Bloom et al. 2005).

In the cytoplasm, sulfate is further processed by ATP sulfurylase, a trifunctional enzyme complex consisting of two polypeptide chains, the sulfurylase CysD and a GTPase CysN (**Fig. 5**) (Schelle & Bertozzi 2006). In *Mtb* CysN carries the APS kinase, CysC, as its C-terminal domain (Sun, Andreassi et al. 2005). ATP sulfurylase can either produce APS, which is the starting material for the reductive branch of the sulfur assimilation pathway subsequently leading to the synthesis of L-cysteine and MSH (Williams, Senaratne et al. 2002). Alternatively ATP sulfurylase can produce PAPS, the substrate for sulfotransferases to produce sulfolipids, membrane components that have been shown to be associated with increased mycobacterial virulence (Goren, Brokl et al. 1974). In particular sulfolipid 1

(SL-1), which is only found in pathogenic strains of *Mtb* (Mougous, Green et al. 2002), is likely to regulate growth inside host macrophages and may provide host specificity (Gilmore, Schelle et al. 2012). In addition SL-1 interferes with superoxide release in macrophages by blocking gamma interferon activation (Rivera-Marrero, Ritzenthaler et al. 2002) and its precursor sulfolipid 1278 triggers a strong immune response in infected patients (Gilleron, Stenger et al. 2004).

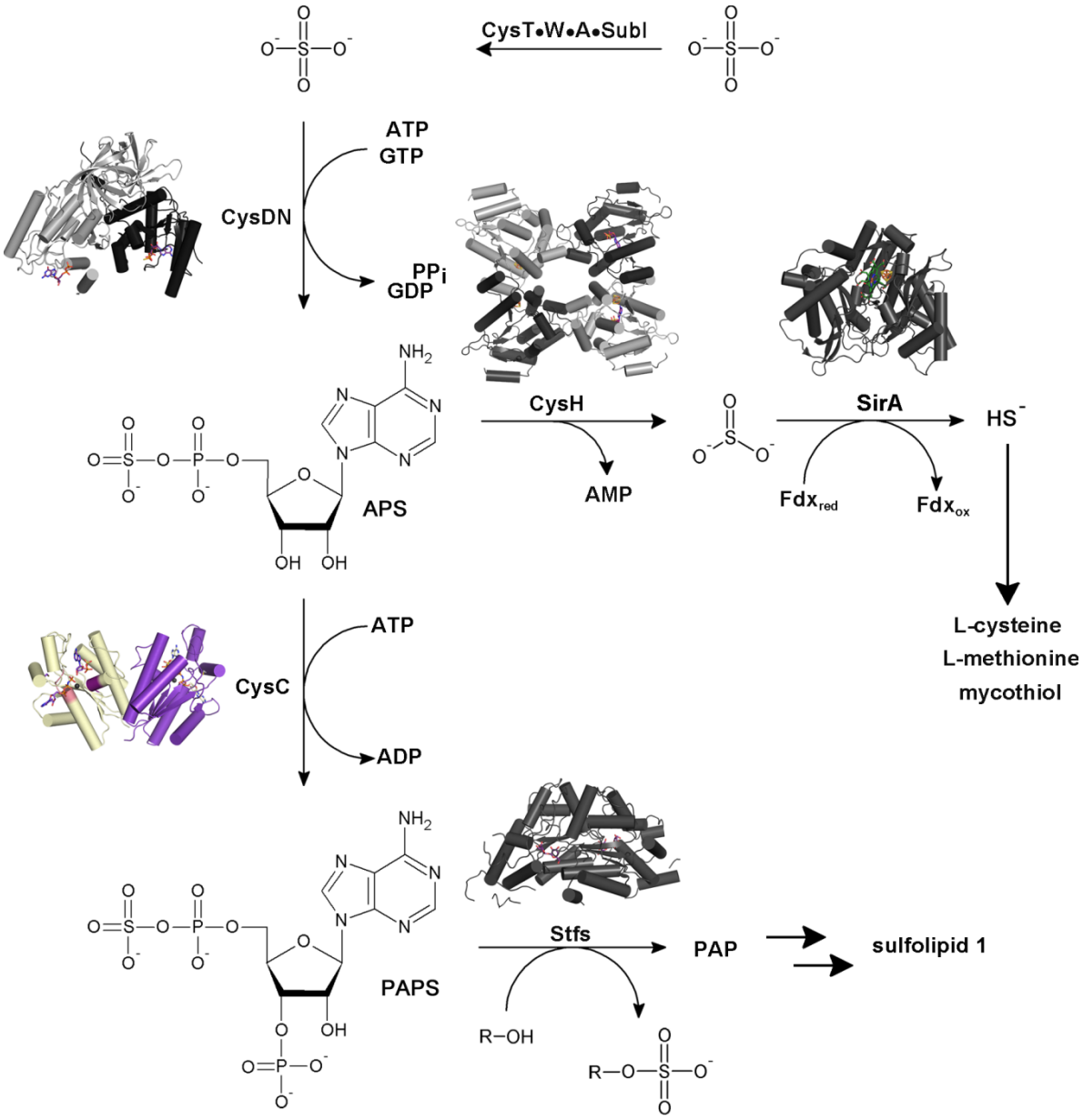

Figure 4. Sulfur assimilation pathway in *Mtb*. After import via a sulfate importer (CysT●W●A●SubI), ATP sulfurylase catalyzes the reaction to either APS (CysD●N) or PAPS (CysC). The reductive branch of the sulfur assimilation pathway continues with reduction of APS to sulfite by APS reductase (CysH). SirA produces sulfide which is then used for biosynthesis of L-cysteine, L-methionine and mycothiol. PAPS is used in the sulfation branch of the sulfur assimilation pathway and serves as substrate for sulfotransferases to produce sulfated metabolites, including sulfolipids. Crystal structures are shown for CysD●N from *Pseudomonas syringae* (PDB 1ZUN), CysH from *Pseudomonas aeruginosa* (PDB 2GOY). Structures for SirA (PDB 1ZJ8), CysC (PDB 4BZX) and Stf0, (PDB 1TEX) are all from *Mtb.* Adapted from (Schelle & Bertozzi 2006).

The remnant of the sulfotransferase reaction is 3'-phosphoadenosine-5'-phosphate (PAP), which is processed by CysQ, a PAP phosphatase hydrolyzing PAP to adenosine monophosphate, and phosphate (Hatzios, Iavarone et al. 2008), which in addition is a competitive inhibitor of sulfotransferases. Alternatively CysQ also uses PAPS as a substrate, resulting in the formation of APS (Pi, Hoang et al. 2005). Disruption of *cysQ* in *Mtb* resulted in a phenotype comprising reduced growth in liquid culture. In these mutants the content of reduced sulfur species remained the same, however presence of SL-1 and its precursor were significantly less abundant compared to the wild type (Hatzios, Schelle et al. 2011).

If APS is utilized for L-cysteine production, the pathway is directed towards the production of reduced sulfur. The first step of the reductive branch is performed by CysH, also called APS reductase which catalyzes the reduction of APS to sulfite and AMP. The necessary reduction potential is provided by the co-factor thioredoxin. The catalyzed reaction follows a two-step mechanism in which APS undergoes a nucleophilic attack, yielding a thiosulfonated enzyme intermediate (Carroll, Gao et al. 2005). The enzyme contains an iron sulfur cluster, which is essential for catalysis, but its exact function is not fully understood. Most likely, it plays a role in sulfuryl group transfer through formation of a electrostatic bridge to the sulfate group of APS and by orienting the catalytic residues and activating the substrate. (Bhave, Hong et al. 2011). In the second step sulfite is released in a thioredoxin dependent manner (Carroll, Gao et al. 2005).

The produced sulfite is then further reduced via a six electron transfer reaction by sulfite reductase SirA, previously denoted NirA (Schnell, Sandalova et al. 2005; Pinto, Harrison et al. 2007). Reduced ferredoxin binds temporarily and delivers electrons via the iron sulfur cluster to the siroheme group to sulfite, which thereby is reduced to sulfide (Kuznetsova, Knaff et al. 2004; Schnell, Sandalova et al. 2005).

1.7.1 The sulfur assimilation pathway in other organisms

The sulfur assimilation pathway in *Mtb* is most similar to the corresponding pathway in the higher plant *Arabidopsis thaliana*, which follows the same steps from sulfur uptake by a transporter via activation as APS to follow the reductive branch of the pathway towards sulfite or as PAPS towards the sulfation branch (Takahashi H 2011; Ravilious and Jez 2012).

Another organism in which sulfur assimilation is well characterized is the γ-proteobacterium *Escherichia coli*. The major difference to *Mtb* is that APS kinase is not fused to the C-terminus of CysN, but expressed as a single polypeptide chain. Instead of employing APS that is reduced by APS reductase to sulfite, in *E. coli* the sulfite that eventually is incorporated in L-cysteine is produced from PAPS by the aid of PAPS reductase (Carroll, Gao et al. 2005). Furthermore the genome of *E. coli* does not encode the necessary genes for PAPS-dependent sulfotransferases that are present in many plants and other bacteria (Sekowska, Kung et al. 2000; Carroll, Gao et al. 2005). To produce sulfated metabolites *E. coli* is dependent on aryl sulfate sulfotransferases that transfer sulfuryl groups from phenolic esters to phenol (Malojčić, Owen et al. 2014).

1.7.2 The mycobacterial sulfate activation complex

In the trifunctional sulfate activation complex (**Fig. 5**) CysD catalyzes the adenylyl transfer from ATP to activate the inorganic sulfate. The sulfate ion performs a nucleophilic attack on the α-phosphorous of ATP to synthesize adenosine 5'-phosphosulfate. The formation of the anhydride bond in APS is energetically disadvantageous, therefore APS production is linked to energy-providing GTP hydrolysis, catalyzed by CysN (Sun, Andreassi et al. 2005).

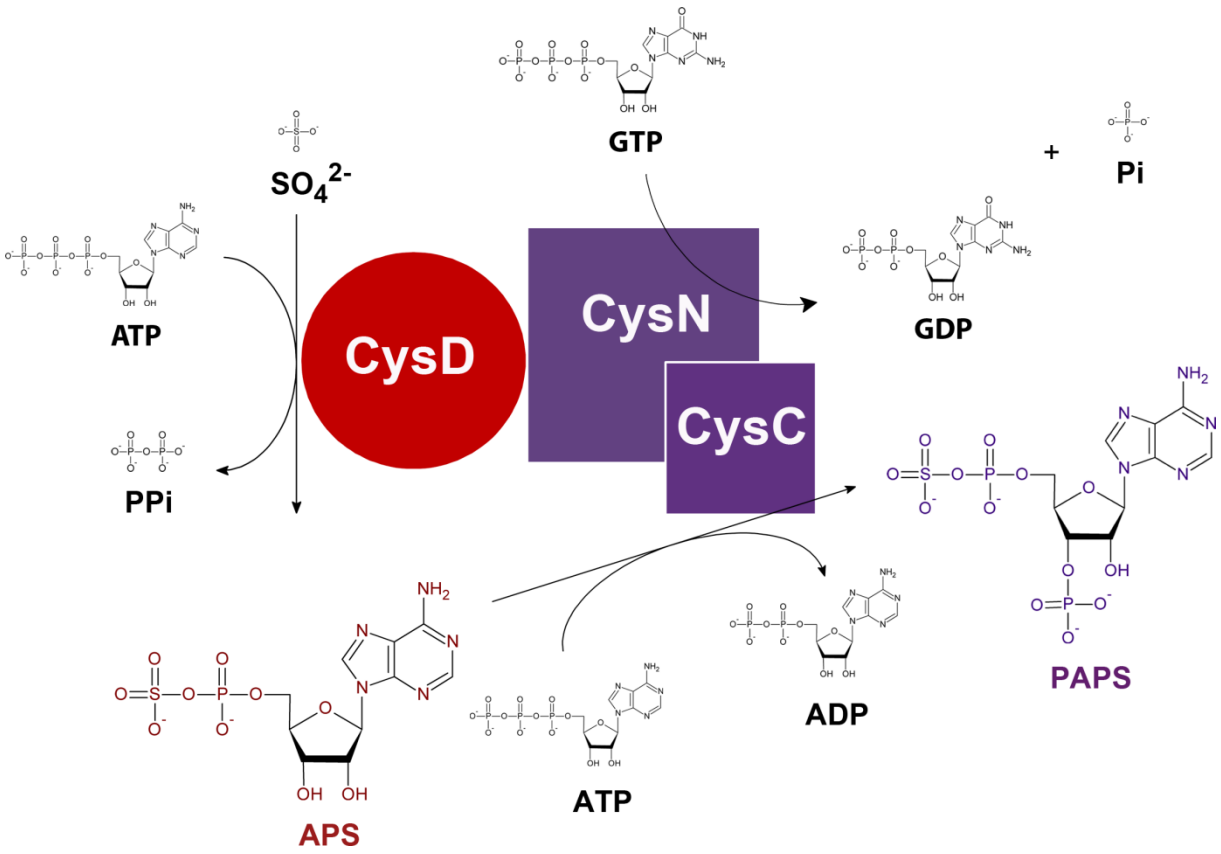

Figure 5. Model of the trifunctional ATP sulfurylase with substrates and products formed. CysD performs the formation of APS from SO_4^{2-} and ATP, which is subsequently used for L-cysteine production. CysN provides the necessary energy to build the sulfuric phosphoric acid anhydride bond in APS by hydrolyzing GTP. CysC, which is fused to the C-terminus of CysN phosphorylates APS to PAPS, which is then used as substrate for sulfotransferases.

ATP sulfurylase lies at a metabolic crossroad that can either direct produced APS towards the reductive branch of the pathway, resulting in the *de novo* biosynthesis of L-cysteine (Schnell, Sriram et al. 2015) and subsequently mycothiol (Jothivasan & Hamilton 2008), or towards the sulfation branch by production of PAPS by CysC. In *Mtb*, the formation of PAPS by CysC is almost 6000 fold more efficient than the formation of APS by CysD, which has been shown by enzymatic studies of ATP sulfurylase *in vitro* (Sun, Andreassi et al. 2005).

1.7.3 APS kinase

The APS kinase domain of mycobacterial ATP sulfurylase, denoted as CysC, has a molecular weight of 21 kDa (Poyraz, Brunner et al. 2015) and belongs to the fold-class of P-loop NTPases. Common in all P-loop NTPases is the presence of the Walker A motif, also known

as the P-loop comprising a consensus sequence of GxxxxGK. For a sequence alignment of CysC with its closest structural homologs, see paper I, Fig. 2. The P-loop is responsible for binding the β-phosphate of the substrate ATP (Leipe, Koonin et al. 2003). In CysC of *Mtb* this loop can be found between β1 and α1 and starts with G450, however with an additional fifth residue between the two glycine residues in the consensus sequence followed by a conserved serine residue, which coordinates Mg^{2+} (Poyraz, Brunner et al. 2015). The Walker B motif is the second characteristic of P-loop NTPases and can be found at the C-terminal end of a hydrophobic β-strand and coordinates the divalent metal ion Mg^{2+} that in turn coordinates the β- and γ-phosphate of ATP, comprised by D478 in the mycobacterial CysC. (Leipe, Koonin et al. 2003; Poyraz, Brunner et al. 2015). The loop region, from residue L477 to D480, found between β2 and α2 is conserved in APS kinases (Poyraz, Brunner et al. 2015).

In many organisms the APS kinases are highly conserved, however, they can be expressed as a single polypeptide chain instead of a fusion protein (Hell 2008), which is the case in *E. coli*. In *Pseudomonas aeruginosa* CysN and CysC are as well fused, but one additional copy of CysC is expressed as a single polypeptide chain (Williams, Senaratne et al. 2002). The APS kinase of *Mtb* shares a high degree of sequence identity with several APS kinases from different organisms, amongst these are the two human homologs PAPS synthetase 1 and 2. The overall sequence identity between mycobacterial CysC and the kinase domains of both human PAPS synthetases is approximately 50%. In contrast to *Mtb*, the APS kinase domain and the adenylyl transferase domain form one bifunctional enzyme on a single polypeptide chain in humans, the APS kinase domain however is found at the N-terminus. The energetically unfavorable phosphoric-sulfuric anhydride bond formation in APS is driven by the separate enzyme, inorganic pyrophosphatase by hydrolysis of PPi (Venkatachalam 2003).

Penicillium chrysogenum APS kinase follows a sequential ordered reaction mechanism in which ATP has to bind before APS and PAPS has to be released before ADP can leave the active site (Renosto, Seubert et al. 1984). APS leads to uncompetitive substrate inhibition in *P. chrysogenum*, *A. thaliana*, human and rat APS kinase, during which the enzyme is trapped in a dead end complex in which ADP and APS are bound in the active site interfering with the sequential ordered mechanism and leaving the enzyme inactive (Lansdon, Fisher et al. 2004).

In *E. coli* the usually followed sequential ordered reaction mechanism can alternatively follow a ping pong mechanism during which a phosphorylated enzyme intermediate at S109 is produced, which is situated between the two nucleotide binding sites. In the presence of low APS concentration the ternary CysC●ATP●APS complex is not formed (Satishchandran & Markham 1989). Later it was shown that the phosphorylated S109 can participate in either of the two reaction mechanisms (Satishchandran, Hickman et al. 1992; Satishchandran & Markham 2000).

In *A. thaliana*, four isoenzymes of APS kinase can be found, which are expressed as single polypeptide chains, however comprise different sizes, the smaller variant with 23 kDa for cytoplasmic expression and a larger variant of 32 kDa, which is a pre-protein, carrying a large transit peptide for export. In addition, in all isoenzymes six conserved L-cysteine residues are found. In APS kinase 1, four of these L-cysteine residues are in close proximity that potentially can form two disulfide bonds. Isoform 1 is activated in the presence of thiols and

thioredoxin, whereas the presence of oxidants results in the opposite, hence it was proposed that activity is dependent on the redox state of these L-cysteine residues (Lillig, Schiffmann et al. 2001). APS kinase 1 and 2 produce the majority of PAPS, which is used for sulfation to produce glucosinolates, essential in plant defense mechanisms (Halkier & Gershenzon 2006). Mutant studies showed that APS kinase 1 would be sufficient for normal growth and APS kinase 3 and 4 are functionally redundant. APS kinase 2 however was shown to be essential for *A. thaliana* germination, because its absence results in inviable pollen (Mugford, Matthewman et al. 2010). Extensive ITC studies of APS kinase 1 confirmed the proposed sequential ordered mechanism. Although binding of APS as the first substrate would be possible and lead to catalysis, the reaction would be slower, because initial ATP binding results in proper positioning of the γ-phosphate in close proximity to the acceptor hydroxyl group in APS and assures the prerequisites for catalysis, by providing optimal conformations of the active sites (Ravilious & Jez 2012).

1.8 *DE NOVO* L-CYSTEINE BIOSYNTHESIS

In *Mtb* three *de novo* L-cysteine biosynthesis pathways are known (**Fig. 6**). The key players are the three PLP-dependent L-cysteine synthases, CysK1, CysM and CysK2, each of them is characteristic for one pathway (Schnell, Sriram et al. 2015). Although all three enzymes produce L-cysteine, they show clear differences in their substrate preference. While CysM and CysK2 use *O*-phospho-L-serine (OPS) as their preferred acceptor substrate, CysK1 exclusively uses *O*-acetyl-L-serine (OAS) (Ågren, Schnell et al. 2008; Steiner, Böth et al. 2014; Schnell, Oehlmann et al. 2007; O'Leary, Jurgenson et al. 2008). CysK1 and CysK2 utilize the sulfide provided by the reductive branch of the sulfur assimilation pathway (Steiner, Böth et al. 2014; Schnell, Oehlmann et al. 2007). CysM is dependent on a small sulfur delivering protein CysO that is thiocarboxylated at its C-terminus (O'Leary, Jurgenson et al. 2008). The three L-cysteine synthases show a sequence identity of approximately 30% with each other and they have been shown to be active during different metabolic states of *Mtb*. While CysK1 represents the classical pathway that is also found in other organisms, such as bacteria (Kredich, Hulanicka et al. 1979; Rabeh & Cook 2004) and higher plants (Bonner, Cahoon et al. 2005), the underlying genes of the two alternative pathways *cysM*, *cysO* and *cysK2* are upregulated under conditions mimicking dormancy, such as hypoxia and oxidative stress (Schnappinger, Ehrt et al. 2003; Voskuil, Visconti et al. 2004; Betts, Lukey et al. 2002; Hampshire, Soneji et al. 2004). Randomized transposon mutagenesis resulted in attenuated mutants deficient in CysO and CysM in an *in vitro* model of dormancy and a mouse model of tuberculosis infection, which lead to the conclusion that the pathway based on CysM is the major route to L-cysteine during dormancy (Rengarajan, Bloom et al. 2005; Sassetti & Rubin 2003). Mammals including humans produce L-cysteine from L-methionine. L-methionine undergoes SAM-dependent transmethylation followed by transsulfuration to yield L-cysteine. L-methionine is an essential amino acid that mammals need to acquire from their diet (Stipanuk 2004).

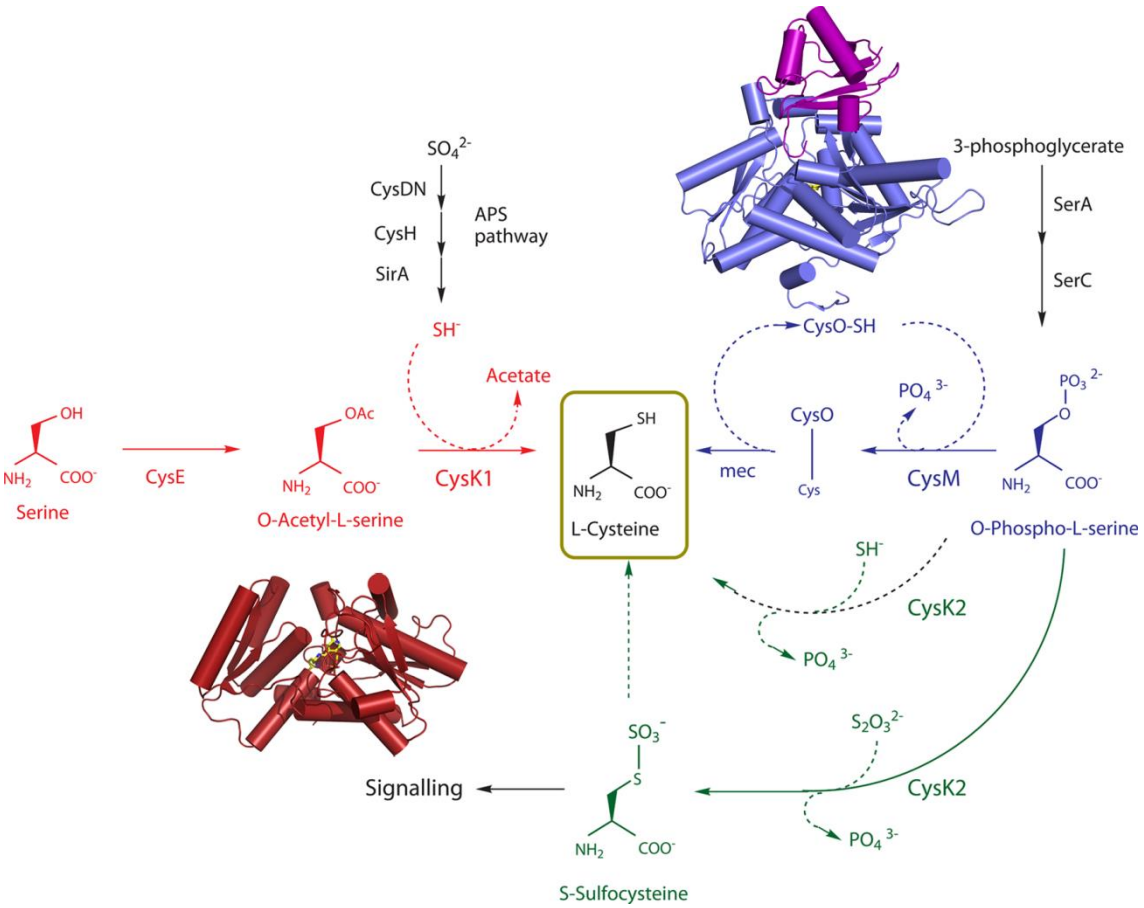

Figure 6. The three routes of *de novo* L-cysteine biosynthesis in *Mtb*. Each route is characterized by one cysteine synthase. In the classical pathway which is shown in red CysK1 utilizes sulfide from the reductive branch of the sulfur assimilation pathway and *O*-acetyl-L-serine (OAS) produced by CysE. In the salvage pathway CysK2 produces L-cysteine from the same sulfur source as CysK1 but uses *O*-phospho-L-serine (OPS) as its acceptor substrate. The preferred reaction of CysK2 however is the formation of *S*-sulfocysteine from OPS and thiosulfate. L-cysteine formation during dormancy is performed by CysM that uses thiocarboxylated CysO as the sulfur donor and OPS. Crystal structures of CysK1 (PDB 2Q3C) and the CysM•CysO complex (PDB 3DWG) are shown in red and blue and purple, respectively. Adapted from (Schnell, Sriram et al. 2015)

1.8.1 The classical pathway to L-cysteine

The classical pathway which is found in most bacteria and plants involves two enzymatic reactions (Campanini, Benoni et al. 2015). CysE first catalyzes the reaction to produce OAS followed by the formation of L-cysteine by CysK1, a *bona fide* *O*-acetyl-L-serine sulfhydrylase (Rabeh & Cook 2004). CysE catalyzes acetylation of L-serine utilizing acetyl-CoA leading to OAS. The C-terminal end of CysE plays an important role in regulation of L-cysteine formation. CysE is active in complex with CysK1, often referred to as L-cysteine synthase complex in the literature (Campanini, Speroni et al. 2005). While CysE is catalytically active, CysK1 remains inactive. Upon complex formation the C-terminal end of CysE is inserted into the active site of CysK1 blocking the binding site for OAS, leading to inhibition of CysK1 (**Fig. 7B**). Increasing concentration of OAS in the presence of reduced sulfur results in dissociation of the complex allowing CysK1 to become catalytically active and produce L-cysteine, while CysE becomes inactive (Campanini, Speroni et al. 2005)

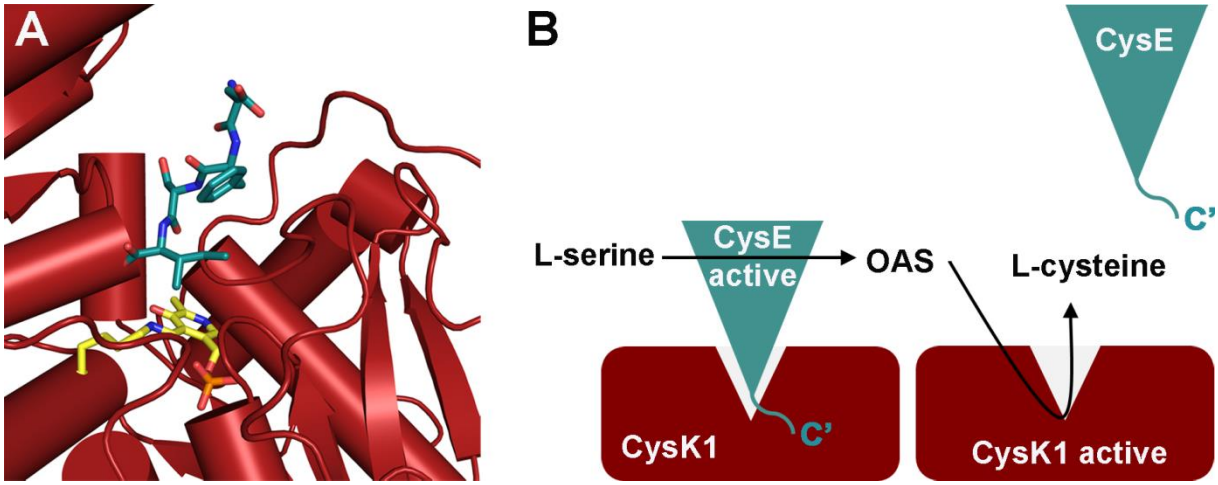

Figure 7. Complex formation between CysK1 and CysE, and the regulation of cysteine biosynthesis. **A)** Magnification of the active site of CysK1 (PDB 2Q3C) colored in red with the inserted C-terminal tetrapeptide DFSI of CysE colored in turquois**. B)** Model of the interplay between CysK1 and CysE. CysE is active while in complex with CysK1 and produces L-serine. When OAS starts to accumulate, the complex dissociates and CysK1 catalyzes L-cysteine formation. Adapted from (Schnell, Sriram et al. 2015).

CysK1 belongs to the fold family of type II PLP-dependent enzymes (Schneider, Käck et al. 2000), with an overall structure divided into two domains, where each shows a typical α/β fold. The domain at the N-terminus is made up by a four stranded parallel β-sheet, which is flanked by three α-helices at one side and one α-helix on the other side. The domain at the C-terminus comprises a mixed β-sheet consisting of six β-strands that are surrounded by four α-helices. The cofactor PLP is bound between the two domains. The enzymatic reaction can be divided into two half reactions following a ping-pong mechanism (Rege, Kredich et al. 1996). In the ground state of CysK1, the PLP cofactor forms an internal aldimine with the catalytic residue K44 via a covalent bond. The first half reaction starts with the formation of an external aldimine between the incoming substrate OAS and the co-factor PLP. CysK1 performs an elimination reaction at the β-carbon position by abstracting one proton at the α-position and releasing the acetate moiety yielding the α-aminoacrylate intermediate and protonated K44 as the product of the first half reaction. The second half reaction is initiated by a nucleophilic attack of sulfide on the β-carbon of the α-aminoacrylate intermediate. Reprotonation of the α-carbon by K44 and release of L-cysteine regenerate the initial ground state of CysK1 (Schnell, Oehlmann et al. 2007).

The classical route of *de novo* L-cysteine biosynthesis is strictly regulated at three levels, which has been demonstrated in *Salmonella*. At the first level, gene expression is under control of CysB, a LysR-type transcription factor controlling gene transcription of the entire cysteine regulon *cysPUWAM* (*cysM* in *E. coli* and *Salmonella* most likely corresponds to the mycobacterial *cysK2* gene). However the genes that are not controlled by CysB are the underlying genes of CysE and CysK1. The product OAS of the CysE catalyzed reaction is prone to non-enzymatic rearrangement to *N*-acetyl serine (NAS). Rising of the NAS level activates CysB and induces transcription of the genes in the cysteine regulon. In contrast

sulfide and thiosulfate act as anti-inducers of gene expression. The second level of regulation is through competitive feedback inhibition of CysE through increasing L-cysteine concentration triggering a rearrangement of the C-terminus that subsequently blocks the binding site of acetyl CoA. The third level is the regulation of the CysE●CysK1 complex formation itself. High OAS concentration leads to dissociation of the complex. Binding of OAS in the active site of CysK1 directly competes with binding of the C-terminal end of CysE comprising the amino acids DFSI in the mycobacterial enzyme. The C-terminal end of CysE in other organisms follows the consensus sequence N, X1, X2, I where X1 corresponds to an aromatic residue and X2 to a strong hydrogen bond donor (Campanini, Benoni et al. 2015). The highly conserved isoleucine at the C-terminal end of CysE probably induces the closing of the active site of CysK1 (Zhao, Moriga et al. 2006; Raj, Mazumder et al. 2013; Huang, Vetting et al. 2005). The tetrapeptide DFSI, which was derived from the C-terminus of mycobacterial CysE was shown to act as a strong inhibitor of CysK1 (Schnell, Oehlmann et al. 2007). From the co-crystal structure it can be seen that DFSI is bound between the two domains of CysK1. The carboxylate group of isoleucine is anchored in the interior of the active site by the conserved residues T71, N74, S72 and Q144 usually binding the carboxylate group of the substrate OAS, whereas the residual amino acids of the tetrapeptide fill the active site pocket (**Fig. 7A**). The conserved residues binding the substrate form part of a loop that with two additional loops between β5 and α3 and β6 and α4, close over the active site upon domain rotation caused by the formation of the α-aminoacrylate reaction intermediate complex. Upon binding of the C-terminal tetrapeptide of CysE, domain rotation is prevented and the active site is blocked (Schnell, Oehlmann et al. 2007).

Paralogs of CysK1 have been shown to gain moonlighting functions upon pairing up with other proteins via the insertion of the C-terminal residues of the binding partner into the active site of CysK1. CysK1 in *C. elegans, B. subtilis* and *S. aureus* have been shown to alter gene transcription. In uropathogenic *E.coli*, CysK1 is involved in activation of an antibacterial protein toxin that inhibits the growth of neighboring bacteria (Campanini, Benoni et al. 2015).

1.8.2 A salvage pathway to L-cysteine formation

CysK2 is the key player of another potential pathway leading to L-cysteine formation. In contrast to CysK1 and CysM, no crystal structure of the enzyme is available, however CD spectroscopy confirmed a mixed α/β fold and spectrophotometry detected the characteristic absorbance maximum of internal aldimine formation of CysK2 and the co-factor PLP, suggesting that it is also belongs to the fold type II family of PLP-dependent enzymes. CysK2 uses OPS and sulfide as a sulfur donor to produce L-cysteine, however with a very low catalytic efficiency. The preferred sulfur donor is thiosulfate instead, reflected in an almost tenfold increase of affinity and a fivefold higher turnover increase when compared to sulfide. The product of the preferred enzymatic reaction is *S*-sulfocysteine, which has been shown to be a direct precursor of L-cysteine in bacteria and plants. The exact physiological role of *S*-sulfocysteine, however, remains enigmatic. One hypothesis is that thiosulfate is produced as a side product of the sulfur assimilation pathway, due to interfering oxidative stress, when the pathogen is engulfed inside the host macrophages and could then act as a sensing molecule of oxidative stress (Steiner, Both et al. 2014). In *A. thaliana* exposure to light induces oxidative stress in chloroplasts. The *S*-sulfocysteine synthase CS26 produces *S*-sulfocysteine a signal

molecule activating redox defense mechanisms, to cope with oxidative stress (Gotor & Romero 2013). Alternatively *S*-sulfocysteine might act as the storage variant of L-cysteine, due to its lower toxicity towards the bacterial cells in comparison to L-cysteine (Nakatani, Ohtsu et al. 2012).

Based on the unique combination of utilizing OPS and sulfide and the low catalytic efficiency of L-cysteine formation via the CysK2 route, this pathway might play a role as a dormancy-induced salvation pathway rather than a major route to L-cysteine production (Steiner, Böth et al. 2014).

1.8.3 L-cysteine formation during dormancy

An alternative pathway leading to L-cysteine production during dormancy is exclusively found in *Actinobacteria* (Burns, Baumgart et al. 2005). The L-cysteine synthase that is the key enzyme catalyzing the reaction to form L-cysteine in this alternative route is CysM. In contrast to CysK1 that uses OAS as its primary substrate, CysM uses OPS to form the α-aminoacrylate reaction intermediate (Ågren, Schnell et al. 2008). Instead of using sulfide ions provided by the reductive branch of the sulfur assimilation pathway, CysM uses the small sulfur-delivery protein CysO that is thiocarboxylated at its C-terminus as a sulfur donor (Burns, Baumgart et al. 2005; Ågren, Schnell et al. 2008; O'Leary, Jurgenson et al. 2008). It was also shown that CysM is capable of using OAS or OPS, however the rate constant of the reaction is more than 600 times higher with OPS, clearly indicating the substrate specificity (Jurgenson, Burns et al. 2008; Ågren, Schnell et al. 2008; O'Leary, Jurgenson et al. 2008). The overall structure of CysM is similar to CysK1, following the same fold family of type II PLP-dependent enzymes, where K51 forms the internal aldimine with the PLP cofactor in the active site. The active site of CysM compared to CysK1 shows several residues which are different, in particular R220 in CysM, found to be responsible for OPS specificity (Ågren, Schnell et al. 2008). CysM can adapt to an open or closed conformation, as has been seen in several crystal structures (Jurgenson, Burns et al. 2008; Ågren, Schnell et al. 2009). Characteristic for the open conformation is a solvent accessible active site. In contrast, in the closed conformation three loop regions at the entrance of the active site comprise different arrangements and the C-terminus is inserted into the active site, making it solvent inaccessible. The α-aminoacrylate of CysM has a half-life eight times longer than the same reaction intermediate of CysK1. This property is due to the firm closure that depends on the conformation of the C-terminus in order to protect the oxidation sensitive reaction intermediate from damage by hydrogen peroxide and other small nucleophiles. Protection of the reaction intermediate may be relevant for survival of *Mtb in vivo*, to assure L-cysteine production inside the oxidizing environment of host macrophages (Ågren, Schnell et al. 2009).

CysO is a small sulfur carrier protein comprising an ubiquitin-like fold. The core of this protein is a four stranded mixed β-sheet, with an α-helix inserted between β2 and β3 (Jurgenson, Burns et al. 2008). Thiocarboxylation of the C-terminus starts with the acyl-adenylation of a diglycyl moiety by MoeZR, which is subsequently converted by the same enzyme through a sulfane group bound at its C-terminus (Voss, Nimtz et al. 2011).

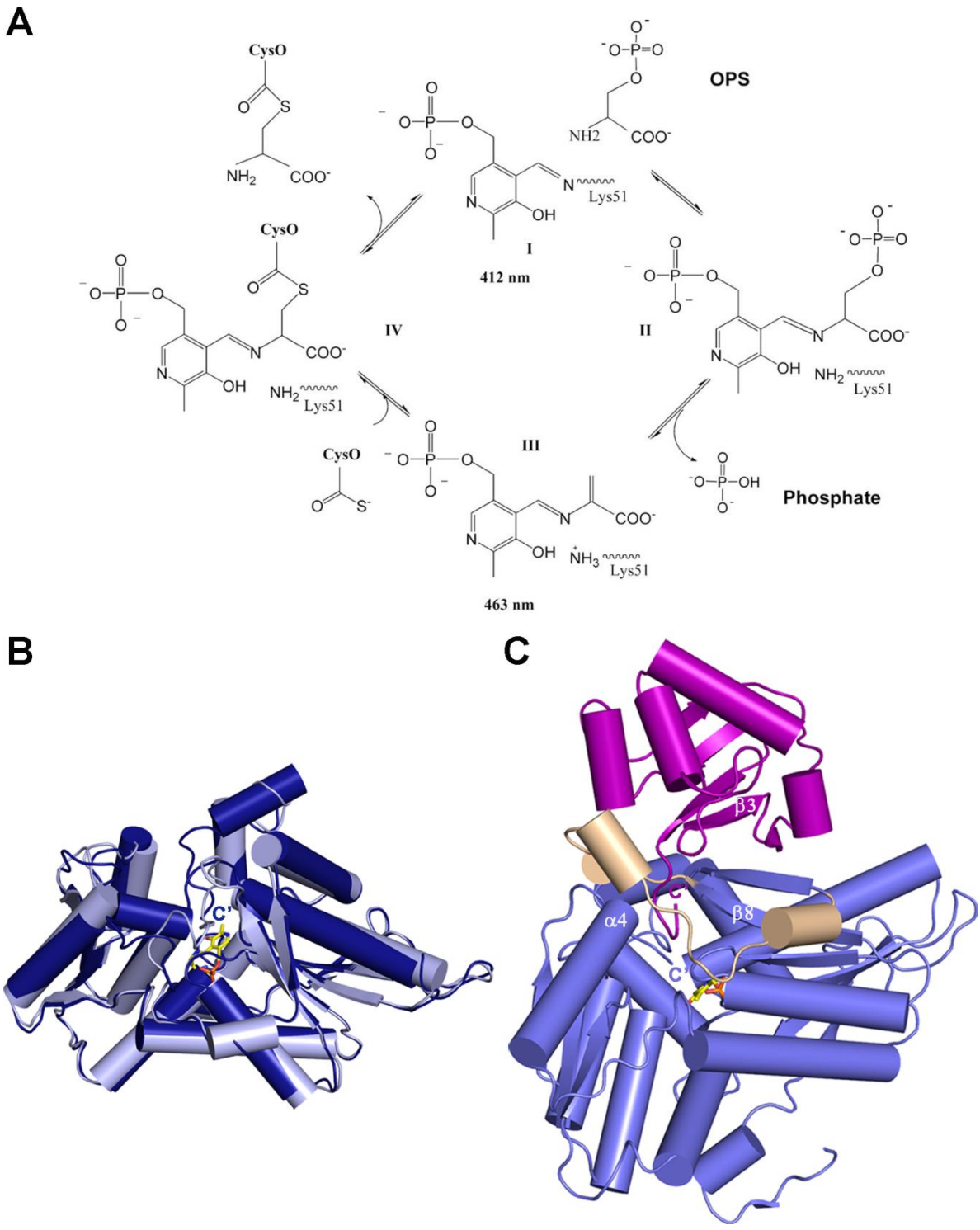

Figure 8. A) Catalytic cycle of CysM indicating the ground state with the internal aldimine formed with K51 (**I**), the external aldimine with the OPS (**II**), the α-aminoacrylate intermediate (**III**), and the CysO-Cys-PLP external aldimine (**IV**). **B)** Superposition of the open and closed conformation of CysM, colored in light and dark blue, respectively. The cofactor PLP is colored in yellow. The C-terminal end of the monomer in the closed conformation is labeled. (PDB 3FGP). **C)** In the CysM●CysO complex, CysM and CysO (PDB 3DWG) are colored in light blue and purple, respectively. Secondary structure elements that are involved in interaction between CysM and CysO are labeled and three 3_{10} helices found in the mobile active site loop (residue 211–237) of CysM are colored in beige.

The overall reaction, catalyzed by CysM, follows a mechanism similar to the CysK1 reaction. (**Fig. 8A**) After conversion of the internal aldimine (**I**) of K51 and the cofactor PLP to an external aldimine (**II**) upon binding of OPS, the phosphate group of OPS is abstracted at the β-carbon via an elimination reaction, yielding the α-aminoacrylate intermediate (**III**). Complex formation between CysM and CysO allows nucleophilic attack on the β-carbon by thiocarboxylate, resulting in a CysO-L-cysteine-PLP adduct (**IV)**. Reprotonation of the α-carbon induces release of CysO carrying the reaction product L-cysteine as a C-terminal adduct, while the initial ground state with the bound internal aldimine (**I**) is restored. Prior to cleavage of the L-cysteine moiety by the zinc dependent metalloprotease Mec^{+}, a spontaneous N-acyl shift in L-cysteine is observed (Jurgenson, Burns et al. 2008). A crystal structure of the CysM●CysO complex comprised an asymmetric CysM dimer, where one monomer adapted to the closed conformation and the second monomer interacted with CysO. The main differences between the two monomers were observed in the loop region stretching from residue 211 to residue 237, which fold into three 3_{10} helices in the CysM●CysO monomer instead of one 3_{10} helix in the closed conformation. In addition part of the N-terminal domain extends away from the core of CysM to allow interaction with CysO. The loop region is also responsible for the majority of interactions with CysO. Other interactions include hydrogen bonding between helix α4 and strand β8 of CysM with a loop region preceding β3 and the C-terminus of CysO, respectively. After β-elimination of phosphate by CysM, the thiocarboxylated C-terminus of CysO is placed into the initial binding pocket of the leaving group of the first substrate (Jurgenson, Burns et al. 2008). Using thiocarboxylated CysO instead of sulfide ions is likely to be beneficial for *Mtb*, especially during dormancy, because thiocarboxylate is more resistant to oxidation and less toxic to the cell (O'Leary, Jurgenson et al. 2008).

In summary, the mycobacterial sulfur assimilation pathway supplies the sulfur required for the production of sulfated metabolites, while the three L-cysteine synthases use sulfur according to their substrate profile. CysM seems to be a dormancy specific L-cysteine synthase and inhibition of CysM is expected to interfere with the availability of mycothiol, crucial for intracellular redox homeostasis.

2 AIMS OF THE THESIS

L-cysteine biosynthesis and the preceding sulfur assimilation pathway have been shown to be essential for *Mtb* in order to maintain its metabolism during active and latent tuberculosis. With this in mind, and with the lack of novel antimycobacterial drugs, we studied four mycobacterial enzymes to determine whether it is possible to discover potent inhibitors with the potential to be further developed into novel antimycobacterial drug candidates.

Paper I – Crystal structures of the Kinase domain of the Sulfate-activating complex of *Mycobacterium tuberculosis*

- Structural and mechanistic characterization of CysC, the APS-kinase domain of mycobacterial ATP sulfurylase
- Comparison to human homologs to evaluate feasibility of developing specific inhibitors targeting the mycobacterial enzyme only

Paper II – Inhibitors of the L-cysteine Synthase CysM with Antibacterial Potency against Dormant *Mycobacterium tuberculosis*

- Performance of a CysM-based HT screening campaign to identify novel inhibitors targeting the L-cysteine synthase CysM, including hit confirmation and hit expansion
- *In vitro* validation of the obtained hits with several orthogonal enzymatic assays and crystallographic methods, including establishment of SAR
- *In vivo* validation of the most potent inhibitors in actively dividing *Mtb* and a nutrient starvation model, reflecting the dormant state of *Mtb*

Paper III – Profiling of *in vitro* activities of urea-based inhibitors against L-cysteine synthases from *Mycobacterium* tuberculosis

- *In vitro* validation of a subset of inhibitors tested during the experiments to generate paper II against the two remaining mycobacterial L-cysteine synthases CysK1 and CysK2 by two orthogonal enzymatic assays
- Identification of inhibitors specific to CysK1 and/or CysK2
- Identification of compounds with triple inhibitory effect against CysK1, CysK2 and CysM

3 RESULTS AND DISCUSSION

3.1 PAPER I – CRYSTAL STRUCTURES OF THE KINASE DOMAIN OF THE SULFATE-ACTIVATING COMPLEX IN *MYCOBACTERIUM TUBERCULOSIS*

The mycobacterial APS kinase domain CysC has been co-crystallized with several nucleotide combinations, ADP alone, ADP and APS and AMP-PNP, a non-hydrolysable analog to ATP, and APS, respectively. Co-crystal structures were solved with the molecular replacement method using the structure of the human PAPS synthetase 1 as a search model (Sekulic, Konrad et al. 2007).

The overall structure of CysC follows the classical α/β purine nucleotide binding fold (**Fig. 9A**) (Schulz, Elzinga et al. 1974). On both sides two α-helices flank the five-stranded parallel β-sheet core. In addition β2 and α2 are connected via one short α-helix and β4 and β5 via two α-helices, respectively. Analytical gel filtration revealed that CysC forms a dimer in solution which is consistent with the crystallographically determined dimeric structure for all three CysC complexes. Analysis of the molecular contacts suggests a buried surface area of 3300 $Å^2$ for the dimer interface formed by helices α2 and α3 with their corresponding symmetry mates.

The closest structural homologs were three bacterial APS kinases from *Aeropyrum pernix*, (PDB 2YVU) , *Thiobacillus denitrificans* (Gay, Segel et al. 2009), *Aquifex aelicus* (Yu, Lansdon et al. 2007), one from the fungus *P. chrysoge*num (MacRae, Segel et al. 2000), one from the plant *A. thaliana* (Ravilious & Jez 2012) and the APS kinase domain from human PAPS synthetase 1 (Harjes, Bayer et al. 2005) with r.m.s.d. values ranging from 0.9-1.5 Å. Sequence identities of CysC with the five homologs ranged from 34 to 52%, sharing the highest sequence identity with human PAPS synthetase 1.

3.1.1 ADP binding site of mycobacterial APS kinase

The ADP binding pocket is found in a cleft that is formed by the conserved P-loop stabilizing the two phosphate groups of ADP on the bottom, loop T551 to K562 followed by helix α5 interacting with the ribose and the adenine base and is completed by the loop formed from L593 to I599 that binds the adenine base on the opposite site. After analysis of the two subunits of the binary complex it became apparent that the ADP molecules are bound in *anti* in two slightly different conformations. The rotation of the glycosidic bond results in a shift of the adenine ring and the α-phosphate. In this complex the major part of the adenine base and the ribose moiety are accessible from the solvent, the bisphosphate group however is tightly fixed to CysC by the P-loop. In the ternary complex CysC●ADP●APS, ADP is bound in one defined conformation and the interactions between ADP and CysC are fully developed as compared to the binary complex. In the second ternary complex, in which ADP was replaced by AMP-PNP in the crystallization mixture, the purine nucleotide binds in the same fashion as ADP. The only difference is the γ-phosphate group that interacts with K456 from the P-loop and K562 on one side and is further stabilized from the opposite site by a bound magnesium cation (**Fig. 9B**).

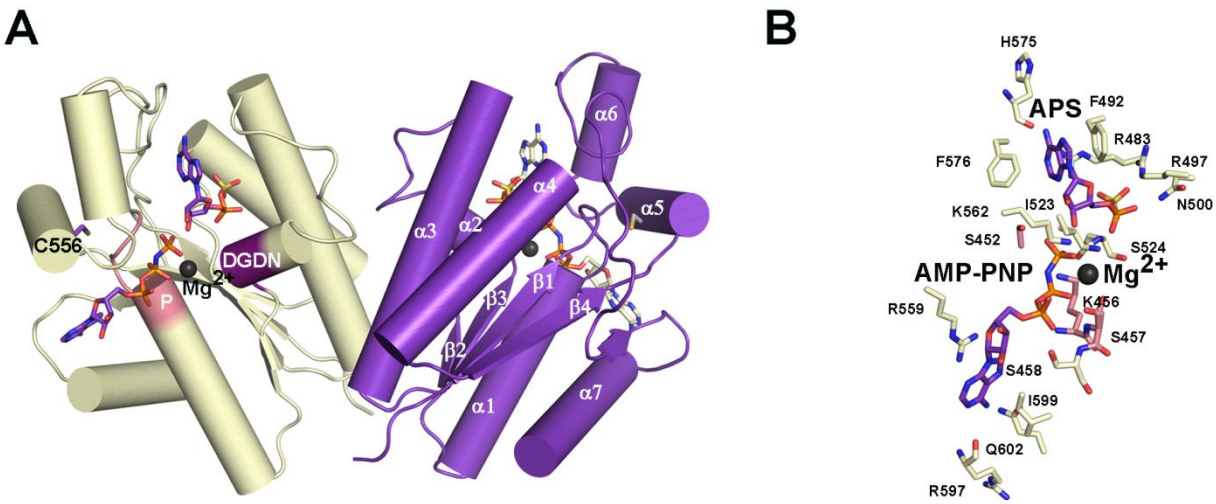

Figure 9. A) Overall structure of the Michaelis complex of the CysC dimer colored in beige and purple with the bound substrates AMP-PNP and APS shown in purple stick representation. The magnesium ion stabilizing the phosphate group is shown as a grey ball. The P-loop is colored in pink and the DGDN loop in purple. The sidechain of C556 is shown in purple stick representation. (PDB 4BZX) **B)** Detailed view of the interactions between CysC and the bound substrates AMP-PNP and APS.

3.1.2 APS binding pocket

The APS binding pocket is found opposite of the ADP/AMP-PNP binding site and formed by loop 490-495 and loop 562-582. APS is oriented with its ribose moiety towards the terminal phosphate group of ADP and AMP-PNP, respectively. The adenine ring of APS is π-stacked between F492 and F576. The former phenylalanine is part of loop 477-499, which is displaced by approximately 2 Å upon APS binding in comparison to the binary complex and thereby closes off the APS binding pocket. Loop displacement explains the relatively high overall r.m.s.d. values of 0.9 Å, between the binary complex and the two ternary complexes, although the protein core retains the same conformation in all three complexes.

3.1.3 Magnesium binding site

In spite of adding Mg^{2+} to the crystallization mixture, no electron density was observed for the divalent metal ion in the ternary complex CysC●ADP●APS. In the second ternary complex CysC●AMP-PNP●APS, where ADP is replaced by AMP-PNP, electron density for Mg^{2+} was observed, which is probably due to the presence of the γ-phosphate in AMP-PNP that contributes to the octahedral coordination of the magnesium ion via its oxygen. The coordination of magnesium is completed by a second oxygen provided by the β-phosphate, the side chain oxygen of S457 and three water molecules.

3.1.4 Mechanistic proposal for phosphoryl group transfer

The ternary complex of CysC in the crystal structure of CysC●AMP-PNP●APS provides a detailed view of the interactions with the substrate and residues that are involved in catalysis and allows a proposal for phosphoryl group transfer (**Fig. 10**). The γ-phosphate of AMP-PNP is in close vicinity of the 3' hydroxyl group of the receiving substrate APS. During catalysis, orientation of AMP-PNP and charge stabilization of its phosphate groups is achieved by the

P-loop and the magnesium ion. Through progression of the enzymatic reaction, a charge accumulation around the γ-phosphate occurs and is stabilized by K562, which is perfectly positioned between the γ-phosphate group of AMP-PNP and the oxygen of 3' hydroxyl group of APS. The conserved residue D480 probably acts as a catalytic base by abstracting a proton from the 3' hydroxyl group of APS, and is attacked by the stabilized γ-phosphate. The mechanism for the APS kinases is preserved in mice, humans, fungi and plants and also CysC follows this mechanism (Singh & Schwartz 2003; Sekulic, Konrad et al. 2007; Lansdon, Fisher et al. 2004; Ravilious & Jez 2012).

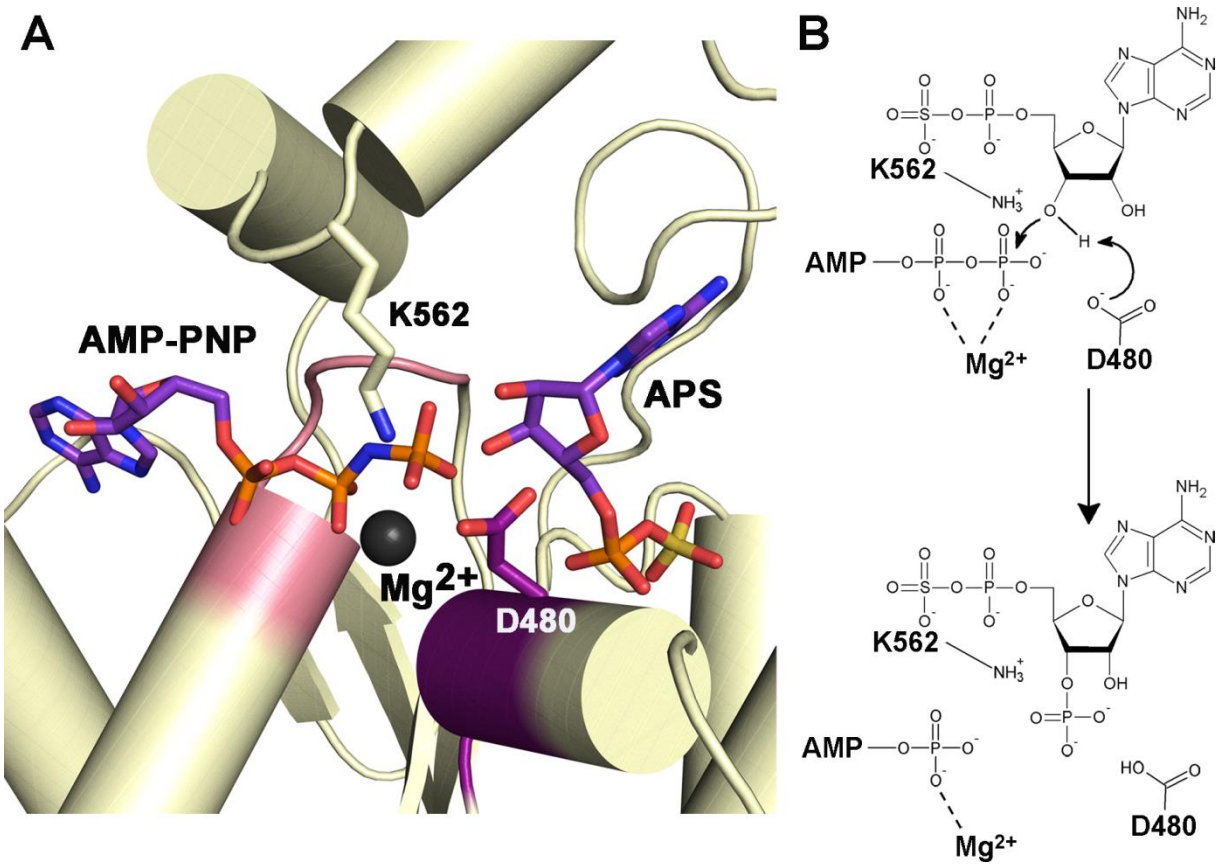

Figure 10. A) Magnification of the CysC active site with bound substrates AMP-PNP and APS shown in purple stick representation and magnesium shown as a grey ball. Residues K562 and D480 which are involved in phosphoryl group transfer are shown in stick representation. (PDB 4BZX) **B)** Proposed mechanism of phosphoryl group transfer in mycobacterial CysC. D480 acts as the catalytic base that abstracts a proton from the 3' hydroxyl group of APS that subsequently reacts with the γ-phosphate of ATP. Charge stabilization during catalysis is achieved by K562.

3.1.5 Comparison to the human PAPS synthetases

PAPS synthetases are the closest human homologs, sharing a sequence identity of approximately 50% with the mycobacterial CysC. Two isoforms have been characterized, PAPS synthetase 1 and 2, which are sharing more than 70% sequence identity with each other (Fuda, Shimizu et al. 2002).

One of the aims of this study was to analyze whether the architectures of the active sites of mycobacterial CysC and the kinase domain in human PAPS synthase 1 and 2 are different

enough to allow inhibitor design to specifically inhibit only the mycobacterial enzyme. Inhibition of CysC would prevent the formation of PAPS, and subsequently would impede formation of sulfated lipids, which is associated with increased virulence in *Mtb* (Williams, Senaratne et al. 2002). The APS binding sites of all three enzymes are very similar. Out of the fifteen amino acids making up the APS binding site, twelve are conserved. An expected increase in binding pocket volume by replacement of A522 (CysC) with F131 (hPAPSS) was minimal. In the loop that binds the adenosine ring of APS T574 and H575 of CysC are exchanged to K183 and G184 in the human enzyme, where only the backbone carbonyl group of K183 participates in interaction with the ligand.

For the ATP binding site, the situation is similar. Although only six out of fourteen residues are conserved, five additional residues comprise similar size and chemical properties as the mycobacterial CysC. Only three amino acids are significantly distinct, which is P561, replaced by V170 in the human homolog, R597 with C/S207 and Q602 with C212. Given the high degree of conserved residues between human PAPS synthetase and CysC the design of specific inhibitors targeting the mycobacterial enzyme only appears to be a challenging task for medicinal chemistry, and was therefore not pursued further.

3.1.6 Is CysC regulated by disulfide bond formation?

During the performance of enzymatic activity assays to demonstrate that mycobacterial CysC is functional as a single unit, it was observed that CysC activity is increased upon addition of reductants, which was also reported for CysC homologs in *A. thaliana* (Sekowska, Kung et al. 2000*)* and *A. aelicus* (Yu, Lansdon et al. 2007). In *A. thaliana* the formation of a regulatory disulfide bond between an L-cysteine in the N-terminal domain and an L-cysteine residue in the core domain of the adjacent monomer was observed. The disulfide bond formation is dependent on the redox state of the surrounding. Reduction results in activation of APS kinase, whereas disulfide bond formation gives a 20-fold less efficient enzyme (Herrmann, Nathin et al. 2015; Lillig, Schiffmann et al. 2001). In the monomer of the mycobacterial CysC three L-cysteine residues can be found, which raised the question if CysC is also regulated upon disulfide bond formation. Five CysC mutants (C514A, C549A, C556A, C556S and a triple mutant, in which all three cysteine residues were mutated to alanine residues) were produced to probe the role of the three L-cysteine residues, since after inspection of the crystal structures it became apparent that none of the L-cysteine residues is involved in the formation of disulfide bonds. Amino acid replacement at position C514 and C549 did result in enzyme variants that show the same activation behavior as the wild type variant, suggesting that neither of these two L-cysteine residues alter CysC activity based on their redox states.

The amino acid replacement at position 556 resulted in a catalytically inactive enzyme. C556S was completely inactive and could not be reactivated upon addition of reductants. The same behavior was observed for the triple mutant. In contrast, the activity of the C556A mutant could be rescued by addition of DTT, but to a smaller extend than it was observed for the wild type. The C556S mutant was sensitive to non-specific proteolysis by thrombin, which was also observed during protein purification of the wild type enzyme. In case of the wild type however, sensitivity could be circumvented by addition of ADP, but not in the case of the C556S mutant.

Co-crystallization of the C556S mutant resulted in a crystal structure with an r.m.s.d. value of 0.5 Å between the mutant and wild type crystal structure of the binary CysC●ADP complex indicating little structural deviations between the two of them. In none of the subunits of the mutant ADP was bound and one segment from residue 552 to 581, including the residue of interest in the C556S mutant, could not be modeled, due to lack of electron density. This stretch belongs to the lid region that closes off the ATP binding site and allows positioning of R559 close to the adenine ring of ATP and is conserved in APS kinases.

Mutagenesis, observed thrombin sensitivity despite addition of ADP and structural analysis indicate that mutation of C556 to S556 results in deficient ATP binding, due to increased flexibility of the lid closing the active site. It is known that enzyme catalysis is linked to protein dynamics. Altered contributions of hydrogen bonds or van der Waals interactions are capable of influencing protein dynamics in such a way that catalysis can be prevented or slowed down (Henzler-Wildman & Kern 2007). Studies on the dynamics of two orthologous adenylate kinases revealed that reduced catalytic activity in one of the kinases could be attributed to slower opening of the lid region (Wolf-Watz, Thai et al. 2004). In CysC the mutation from L-cysteine to L-serine might have a similar effect on the lid closing the ATP binding site, but instead of reducing catalytic activity the enzyme remains entirely inactive. Overall, oxidative stress, caused by macrophages in order to clear *Mtb* infections, might partially oxidize the thiol groups of L-cysteine residues present in CysC and thereby direct sulfur assimilation towards the reductive branch to produce L-cysteine and subsequently mycothiol. Imagining such a type of enzyme regulation would allocate CysC the role of a switch that decides upon the fate of activated sulfate.

3.2 PAPER II – INHIBITORS OF THE L-CYSTEINE SYNTHASE CYSM WITH ANTIBACTERIAL POTENCY AGAINST DORMANT *MYCOBACTERIUM TUBERCULOSIS*

3.2.1 High-throughput screening and selection of hits

To screen for potential hits targeting CysM in a high-throughput format, a target-based approach was chosen. The high-throughput screening assay employed was based on the PLP fluorescence emission signal increase upon binding of compound in close vicinity to the covalently bound PLP cofactor in the active site (Campanini, Speroni et al. 2005). The advantage of the PLP fluorescence emission assay was that it was easily adaptable to high throughput format.

The PLP fluorescence emission assay, however, faces several limitations as screening assay and method to reliably determine K_d values. Compounds that fail to induce significant changes in PLP fluorescence cannot be identified as potential binders. This is particularly true for allosteric inhibitors binding far from the cofactor PLP. Enzymatic assays, using OPS and the small sulfur delivery protein CysO as a sulfur donor to identify inhibitors would be capable of identifying allosteric inhibitors as well, but would meet major obstacles in terms of producing sufficient amounts of pure thiocarboxylated CysO *in vitro*. In addition this assay is not suitable to be adapted to high-throughput format. The sensitivity of the assay limits the range of K_d values that can be determined reliably. The enzyme concentration required to obtain an acceptable signal to background ratio sets a limit for binding constants to the low micromolar range. The used CysM concentration of 2 μM would require the addition of the corresponding concentration of inhibitor to saturate all inhibitor binding sites and hence sets the limit for a K_d value that can be determined to ≥ 1 μM.

Screening of a chemically diverse library, consisting of 17,312 lead- to drug-like molecules against CysM, resulted in the identification of twenty concentration dependent active site binders. After passing the initial hits through filters to remove potential aggregators, unwanted reactive and pan-assay interference compounds (PAINS), six compounds remained. Focus was put on two closely related compounds based on a urea scaffold, because several structural analogs were accessible through the compound library of the screening facility. The PLP fluorescence assay was also employed to determine K_d values of these initial two urea scaffold hits, which were found to be in the low micromolar range.

3.2.2 Hit expansion

Hit expansion was an iterative process, including several rounds of compound selection and synthesis. Insights from co-crystal structures of enzyme-inhibitor complexes, combined with obtained biochemical data from five orthogonal enzymatic assays, guided the design of structural analogs. The compound library used for *in vitro* validation contained 71 compounds, of which 54 were synthesized by our collaborators from BITS-Pilani, Hyderabad, India, and the remaining seventeen were either available through the compound library of the screening facility CBCS or purchased from commercial vendors.

3.2.3 *In vitro* validation

Five orthogonal assays were exploited to characterize the 71 compounds in the prepared compound library to derive structure-activity relationships (SAR). K_d values were determined by exploiting the PLP fluorescence emission assay and wherever necessary due to affinities in the low micromolar range, the alternative method ITC was used. In addition first order rate constants (k_{obs}) of the first half reaction were determined by spectrophotometrically monitoring the formation of the α-aminoacrylate reaction intermediate. Derived k_{obs} values in the presence of 100 µM compound and 500 µM OPS were then compared to k_{obs} values of the uninhibited reaction to determine the remaining activity of CysM. The strongest inhibitors were tested if they fully inhibit the enzymatic reaction of CysM, by preventing the formation of the reaction product L-cysteine-CysO adduct. The reaction products were analyzed by ESI-MS. Compounds **1** and **2** fully inhibited the CysM●CysO reaction, indicated by the presence of only one peak in the MS spectrum, corresponding to the thiocarboxylated CysO. Compound **3** and **5-7**, showed partial inhibition, indicated by the presence of two peaks, one corresponding to the mass of thiocarboxylated CysO only and the other corresponding to the L-cysteine-CysO adduct. Although compound **17** was showing relatively high affinity and decreased CysM activity, only one peak corresponding to the molecular weight of L-cysteine-CysO adduct was detected, indicating that this compound had little potential to inhibit the overall CysM●CysO reaction. Compound **1** was the strongest inhibitor characterized, with an apparent K_d of 0.3 µM, determined by ITC and an IC_{50} value of approximately 0.5 µM of the multiple turnover enzyme reaction using thiocarboxylated CysO as the sulfur donor. Phosphate release after β-elimination from OPS was monitored spectrophotometrically, after derivatization with malachite green reagent to demonstrate the concentration dependency of inhibition on the multiple turnover enzyme reaction. Biochemical data and resolution of the obtained co-crystal structures of the strongest inhibitors are summarized in **Tab. 1** below. Further details on the biochemical data of all tested compounds, and descriptions of the five orthogonal assays, can be found in Tab. 1 in paper II and Tab. S2 and the materials and methods section in the supplementary information of paper II.

Table 1 Summary of the obtained biochemical data for the strongest inhibitors targeting CysM and corresponding resolutions of the complex crystal structures**.**

Compound	K_d (µM)	k_{obs} (min^{-1})	Activity (%)	CysO-CYS	Resolution (Å)
1	0.3 ± 0.01	0.1 ± 0.01	0.3	INH	2.1
2	1.7 ± 0.1	0.24 ±0.06	0.6	INH	1.7
3	4.5 ± 0.2	0.48 ± 0.18	1.2	partial INH	2.7
4	2.2 ± 0.1	0.23 ± 0.05	0.6	n/d	2.0
5	8.0 ± 0.6	1.92 ± 1.08	4.9	partial INH	1.6
6	1.4 ± 0.4	0.48 ± 0.12	1.2	partial INH	2.6
7	3.4 ± 0.1	0.24 ± 0.06	0.6	partial INH	2.5

3.2.4 Crystal structures of the enzyme-ligand inhibitor complexes

The overall structure of CysM in complex with the best inhibitors showed little deviation from the crystal structure of CysM in complex with the external aldimine, as indicated by r.m.s.d values between 0.7–1.4 Å after superposition of the Cα carbons. The fold of type II PLP-dependent enzymes, comprising two domains, where each shows the typical α/β fold, is maintained in all the inhibitor complexes. After manual inspection of the CysM●inhibitor complexes, it became apparent that the open and the closed conformation are observed within the same dimer. The open conformation comprises a disordered C-terminus (residues 310-323) and a disordered mobile active site loop, containing residue R220, which results in an open active site. In the co-crystal structures in which CysM is in complex with the inhibitors, the open conformation allows partial solvent exposure of the inhibitor. In the closed conformation however the active site loop and the C-terminus are well defined and they fold over the inhibitor binding site, preventing solvent exposure. In order to describe the CysM-inhibitor interactions the closed conformation was chosen, in which the active site loop and the C-termini are resolved and hence interactions between CysM and the inhibitors are fully established.

3.2.5 Common features of best inhibitors

The most potent inhibitors share all common structural features and consist of three parts (**Fig. 11A**). The left-hand side (LHS) is always a phenyl ring substituted with a carboxylate group. The LHS is connected via a urea linker to the right-hand side (RHS), which is either a substituted monophenyl. (type I inhibitors, compounds **1**, **5-7**) or a bisphenyl group (type II

inhibitors, compounds **2-4**) (**Fig. 11B-F**). All seven inhibitors bind in the same orientation with their carboxylated LHS, binding in a similar fashion as the carboxylate group of the substrate OPS, as can be seen from the crystal structures of CysM in complex with compounds **1** – **7**. Type I inhibitors interact via hydrogen bonds with the conserved residues T78, S79, N81 and T82 involved in carboxylate group binding of the natural substrate OPS. The characteristic carboxylate group is common in all potent inhibitors identified for the mycobacterial homolog CysK1 and paralogs of L-cysteine synthases in other organisms, such as *H. influenzae* and *S. enterica* (Schnell, Oehlmann et al. 2007; Poyraz, Jeankumar et al. 2013; Salsi, Bayden et al. 2010; Amori, Katkevica et al. 2012; Pieroni, Annunziato et al. 2016). A substitution of the LHS with a tetrazolidine group resulted in complete loss of binding, which further underpins the carboxylate group as a hallmark of inhibitors targeting L-cysteine synthases. It became apparent that introduction of additional substitutions on the LHS of type I inhibitors resulted in decreased binding ability as demonstrated by the introduction of one additional hydroxyl or repositioning of the carboxylate group from *meta* to *para*. Interactions of the carboxylate binding pocket of CysM with the type II inhibitor compound **3**, comprising a carboxylate substituted LHS only involve binding of the conserved residues N81 and T82. In general type II inhibitors are more tolerant towards substitutions on their LHS, as shown by retained binding affinities and no loss in inhibitory power upon introduction of the additional hydroxyl group or repositioning of the carboxylate group, which is due to conformational changes caused by the urea linker in combination with the RHS of type II inhibitors, as can be seen in compound **3** and **4.**

The urea linker forms stacking interactions with PLP, orienting itself in parallel to the plane of the pyrimidine ring of the co-factor in the active site. The carbonyl group of the urea linker interacts via a hydrogen bond with R220, which is part of the mobile active site loop and both amides interact with two internal water molecules in type II inhibitors. In type I inhibitors, the interactions between enzyme and urea linker differ, in fact the carbonyl group of urea interacts with N221, one residue upstream in the polypeptide chain as compared to type II inhibitors. Amide interactions are formed with the terminal residue A323 and one internal water molecule. Exchanging the central linker against thiourea, sulfonamide, amide or an elongated urea group resulted in compounds not binding to CysM.

The RHS occupies a rather flexible hydrophobic pocket that adapts to the different sizes of type I and type II inhibitors, which is due to the high flexibility of the active site loop and the C-terminus that folds over the active site pocket. Binding of type II inhibitors induce a different conformation of the active site loop that increases the size of the hydrophobic binding pocket of the RHS. In addition the different conformation of the active site loop does not allow insertion of the C-terminus into the active site pocket and thus results in differences in interaction with the urea linker (**Fig. 11C** and **11D**).

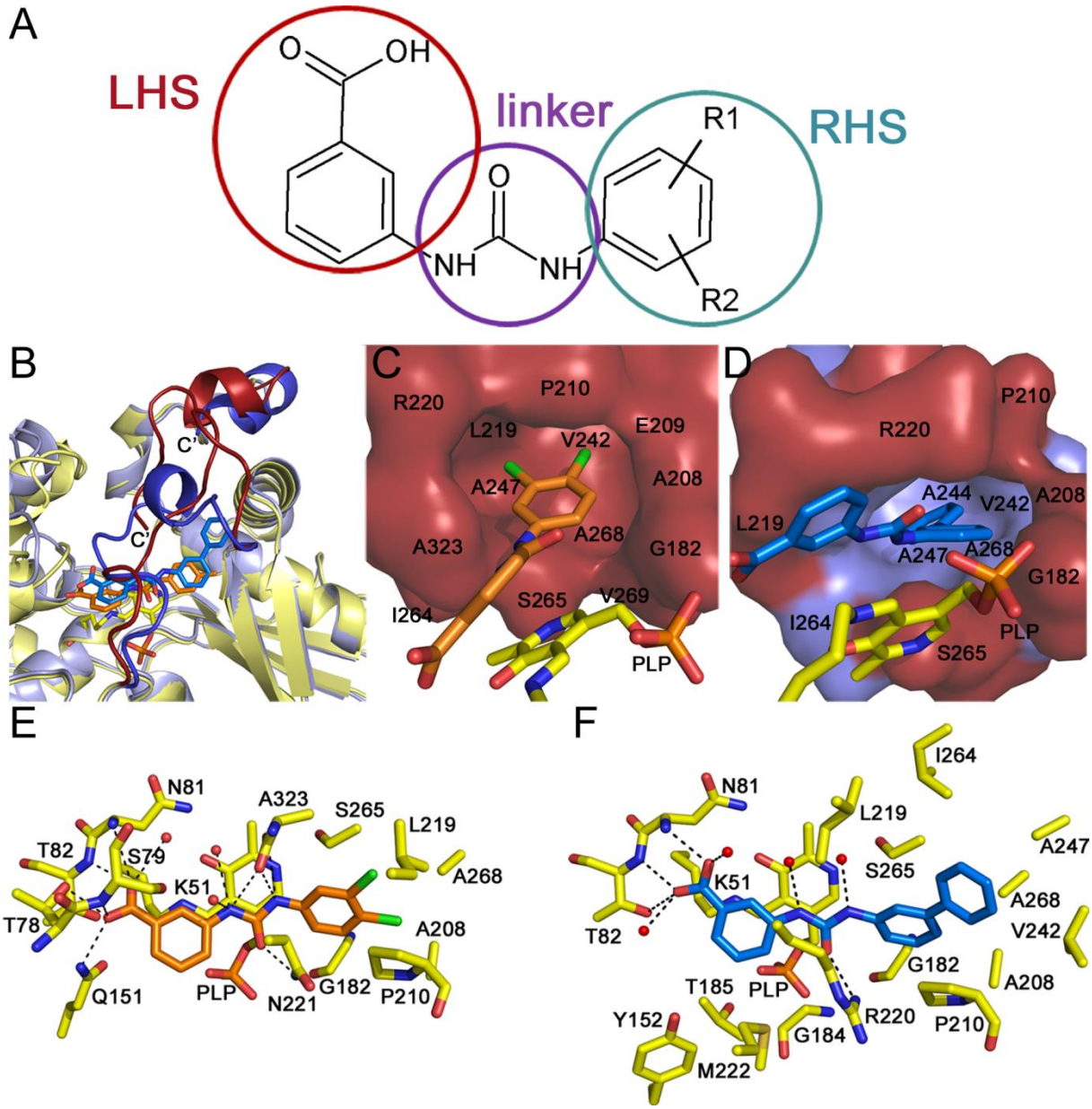

Figure 11. A) General scaffold of the urea-based CysM inhibitors. **B)** Superposition of CysM in complex with compound **5** (PDB 5I6D) and compound **2** (5I7R) showing the two different conformations of the active site loop and the C-terminus upon binding of the two types of the urea-based inhibitors. The complex structure of CysM and compound **5** is colored in yellow and compound **5** is shown in stick representation in orange. The corresponding active site loop and the C-terminus are colored in red. The complex structure of CysM and compound **2** is colored in light blue, compound **2** is shown in stick representation colored in marine and the corresponding active site loop and the C-terminus are colored in dark blue. **C)** Binding pocket of type I inhibitors with compound **1** shown in orange. (PDB 5I7A) **D)** Expanded binding pocket upon binding of type II inhibitors **E)** Detailed interaction of compound **1** with CysM. **F)** Detailed interaction of compound **2** with CysM.

Binding affinity of type I inhibitors were negatively affected by introducing electron withdrawing groups, clearly indicating that halogen substitutions were preferred, as could be seen for the best inhibitor, compound **1**, that is chlorine-substituted in *meta* and *para* position. Type II inhibitors did not allow substitutions on the terminal phenyl group without sacrificing binding affinity. From the co-crystal structures of CysM and compounds **2**, **3**, and **4** it is obvious that binding of type II inhibitors does not allow further size increase of the RHS, due to less than 4 Å of space in either direction.

3.2.6 Antimycobacterial activity of urea-based inhibitors

The strongest inhibitors were tested against actively dividing *Mtb* and showed MIC values between 2-20 µM. In the lower micromolar range, these MIC values are not as potent as MIC values achieved by culture treatment with isoniazid and rifampicin, which were determined to 0.4 µM and 0.5 µM, respectively. However, CysM is expected to be most active during the dormant phase of *Mtb*, therefore a nutrient starvation model was chosen. The conditions in this model reflect conditions inside host macrophages and as a result *Mtb* remains in a non-replicating state. Compound **2** and **5** showed comparable killing activities to the antibiotics rifampicin and moxifloxacin, known to have a killing effect on non-replicating *Mtb*. Compound **1** and **3** even showed improved killing activities over rifampicin and moxifloxacin by decreasing the bacterial count by three orders of magnitude. In order to address whether the observed bactericidal effect was due to targeting of the L-cysteine biosynthesis the cultures treated with compound **1** and **3** were supplemented with L-cysteine and a complete loss of antimycobacterial activity was observed, which hints towards L-cysteine biosynthesis, as the actual target of the identified inhibitors. The inhibitors were tested for cytotoxicity against three human cell lines and one mouse cell line. None of the tested inhibitors showed significant cytotoxicity towards the mammalian cells.

3.2.7 Compound selectivity

A homology search of the human genome identified cystathionine beta synthase as the closest human homolog, with a sequence identity of 29%. The affinity of compound **1** was 300 times lower than for CysM and compound **2** did not bind at all. The low cytotoxicity and the selectivity for CysM over the closest human paralog make the identified set of inhibitors a valuable starting point for developing a drug to specifically target dormant *Mtb*.

3.3 PAPER III – PROFILING OF *IN VITRO* ACTIVITIES OF UREA-BASED INHIBITORS AGAINST L-CYSTEINE SYNTHASE FROM *MYCOBACTERIUM TUBERCULOSIS*

The presence of the two additional L-cysteine synthases in *Mtb* raised the question of whether the identified compounds described in paper II selectively inhibit CysM or also target the two other homologous mycobacterial L-cysteine synthases CysK1 and CysK2. The 71 compounds used for determining SAR for CysM, were rescreened against CysK1 and CysK2 with two orthogonal assays. One assay was based on a fluorescence emission signal increase or decrease upon binding of an inhibitor in close proximity of the PLP-cofactor in the active site (Campanini, Speroni et al. 2005). The second assay was based on the spectrophotometric detection of L-cysteine, the product of the enzymatic reaction, after derivatization with ninhydrin. Traditionally, ninhydrin is used to derivatize amino groups in compounds, such as amino acids. However, if the reaction is performed in acidic milieu the derivatization is specific for L-cysteine and results in the formation of a distinct pink derivative, which can be detected at a wavelength of 560 nm (Gaitonde 1967). The same derivatization method could be used to monitor formation of *S*-sulfocysteine, the reaction product of CysK2, since it was shown that *S*-sulfocysteine also results in the formation of the same pink derivative, due to acidic hydrolysis to L-cysteine and sulfide (Steiner, Böth et al. 2014). For the initial screening of the 71 compounds both assays were exploited to determine the fact of binding and inhibition. For identified hits the PLP-fluorescence-based assay was used to determine K_d values and the assay based on ninhydrin derivatization was used for IC_{50} determination.

3.3.1 Identification of inhibitors targeting CysK1 and CysK2

During screening of the 71 compounds, it became apparent that the PLP-fluorescence-based assay was not sufficient to identify all compounds that also showed inhibition of CysK1 and CysK2. Some of the compounds that did not result in an increase or decrease of fluorescence signal did nevertheless show inhibition of CysK1 and CysK2, and IC_{50} values could be determined. For CysK1 six compounds comprising IC_{50} values between 2.5–29.4 µM were identified, with compounds **9** and **2** being the strongest inhibitors. In the case of CysK2 seven compounds with IC_{50} values between 6.6–29.9 µM were determined. The best inhibitors for CysK2 were shown to be compounds **1** and **2**.

3.3.2 Urea-based compounds inhibit all three mycobacterial L-cysteine synthases

In total, four inhibitors, compounds **1** to **4**, were identified that target both L-cysteine synthases, CysK1 and CysK2 (**Fig. 12**). These compounds were also among the top inhibitors targeting CysM, however, the determined IC_{50} for CysM with compound **1** was 20 times lower than the IC_{50} for CysK1 and CysK2, which were shown to be approximately 10 µM.

All the inhibitors of the L-cysteine synthases identified so far carry a carboxylic acid substitution that interacts with the conserved residues T71, S72, N74, T75 and Q144 (residue numbering based on CysK1) usually binding the carboxylate group of the natural substrates OAS and OPS (Cox & Laessig 2014; Poyraz, Jeankumar et al. 2013; Pieroni, Annunziato et al. 2016; Amori, Katkevica et al. 2012; Salsi, Bayden et al. 2010). The loops, however, which are responsible for closing off the active site, are different in sequence and conformation in

all three L-cysteine synthases and explain the preference of one L-cysteine synthase for a certain inhibitor over the other. The urea-based compounds identified as inhibitors within the frame of this study follow the same pattern, carrying the characteristic carboxylic acid moiety on their LHS. The RHS, however, allows some variation, since both L-cysteine synthases, CysK1 and CysK2, show affinity for both types of inhibitors, the mono-substituted phenyl and the bisphenyl variant. Halogen substituted phenyls show stronger inhibition of CysK2 and CysM. They also inhibit CysK1, but to a much weaker extent.

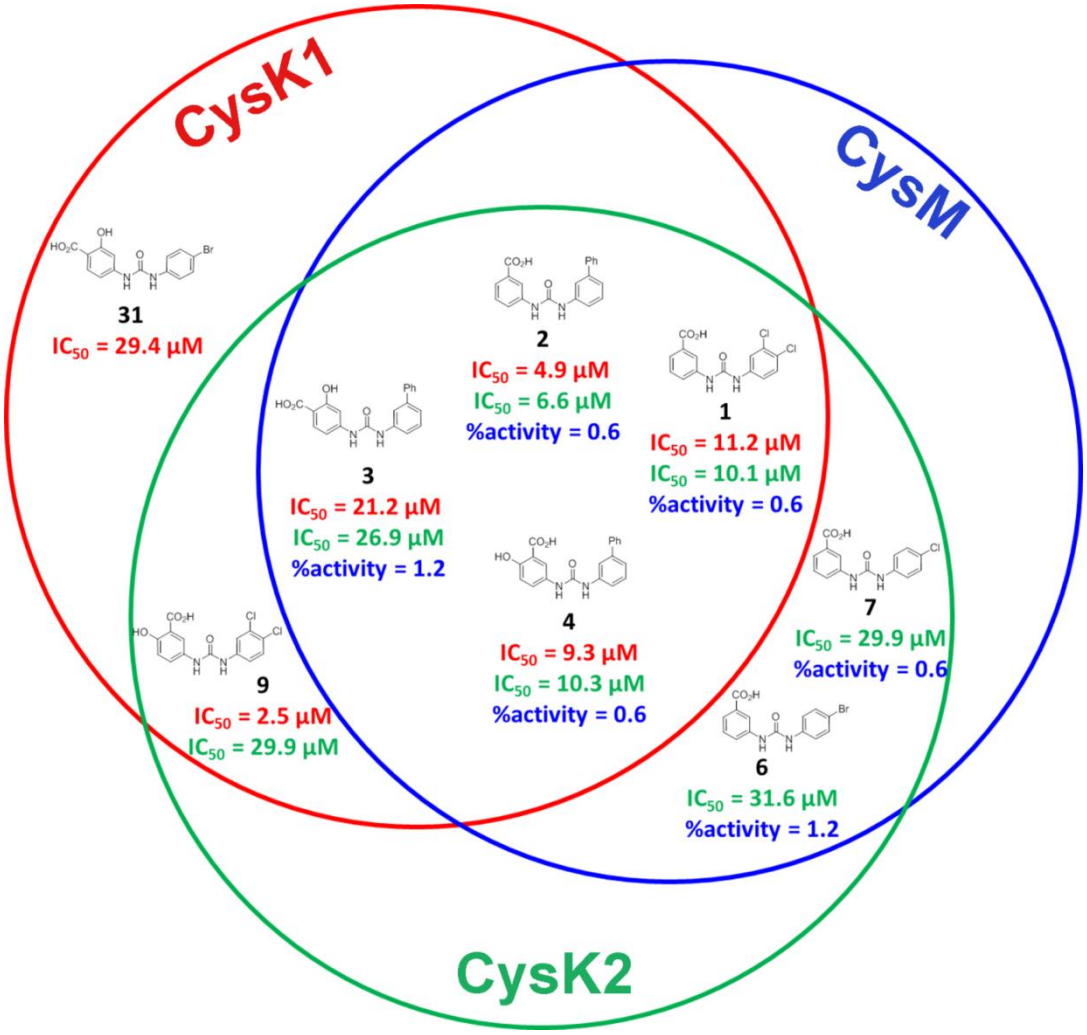

Figure 12. Venn diagram illustrating the inhibitory profile of the urea-based compounds of mycobacterial cysteine synthases. The blue circle represents CysM, the red circle CysK1 and the green circle CysK2. Below the compound structures IC_{50} values for CysK1 and CysK2 are shown in red and green, respectively. For comparative reasons remaining activity in percent for CysM are shown in blue.

In general L-cysteine synthases seem to be tolerant towards the introduction of an additional hydroxyl group, with the exception of compound **9**, belonging to the type I inhibitors of L-cysteine synthases. Compound **9** only inhibits CysK1 and CysK2, but not CysM, indicating that introduction of the hydroxyl group on the LHS of type I inhibitors prevents binding of CysM. This observation is underpinned by the effective binding and strong inhibition of all three L-cysteine synthases by compound **4**, which belongs to type II inhibitors with the same LHS substitutions as compound **9**.

3.3.3 Comparison of the CysK1 specific inhibitors: urea-based scaffold *versus* thiazolidine-based scaffold

To understand the structural basis of selectivity, extensive attempts to generate crystal structures of CysK1 and CysK2 with bound inhibitors were made. Using an established crystallization condition to obtain complex crystals of CysK1 and compounds **2** and **9** resulted in the formation of protein crystals with no inhibitor bound. 96-well HTS in presence of compounds **2** or **9** to identify novel crystallization conditions did not result in any formation of protein crystals. The crystal structure of CysK2 has not been solved yet, although excessive efforts by various researchers in our research group have been made to obtain crystals over the past 10 years. HTS for crystallization conditions for CysK2 in complex with compound **2**, unfortunately, did not result in any formation of well-diffracting crystals.

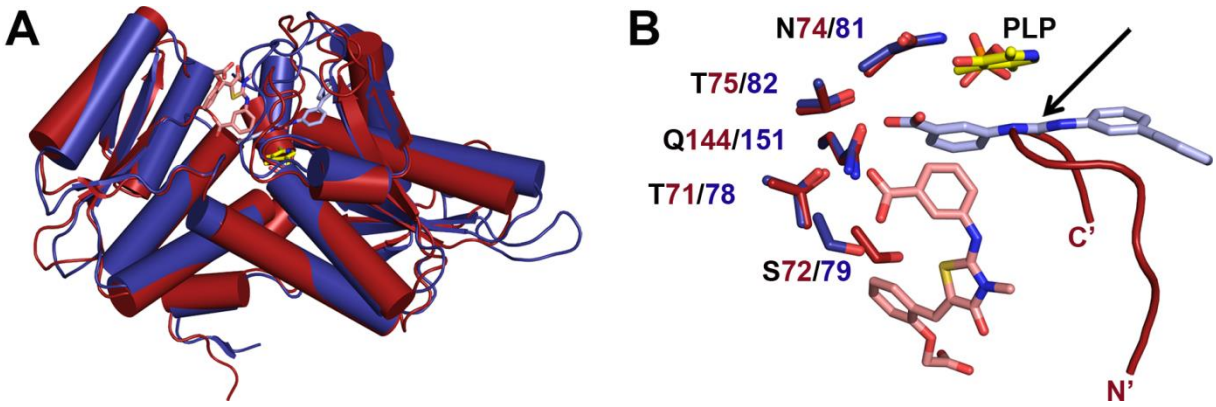

Figure 13. A) Superposition of CysM and CysK1. CysM is colored in dark blue and CysK1 in bordeaux. The PLP-cofactor is colored in yellow, and the thiazolidine inhibitor is shown in pink and compound **2** in light blue. **B)** Magnification of the superposed inhibitor binding sites of CysM and CysK1. Conserved active site residues binding the carboxylic acid moiety of the two inhibitors are shown in stick representation and colored blue and bordeaux for CysM and CysK1, respectively. A loop segment that closes off the active site of CysK1 is shown in bordeaux. Binding of compound **2** by CysK1 in the same orientation as by CysM is not possible, due to severe clashes indicated by the arrow, suggesting that the urea-based compounds bind to CysK1 in a different manner compared to CysM.

Although all potent inhibitors of L-cysteine synthases identified so far carry a carboxylic acid group that is anchored through interactions with highly conserved active site residues, a structural basis to identify more similarities and/or differences in how the inhibitors interact with each of the mycobacterial L-cysteine synthases would be valuable. Understanding which parts of the inhibitors can be modified in order to increase affinity for one target, while not sacrificing it for the other, could potentially result in more potent inhibitors targeting all three L-cysteine synthases at once. Superposition of the crystals structures of CysK1 in complex with thiazolidine, and CysM in complex with compound **2**, shows the potential binding orientation of the urea-based inhibitors in the active site of CysK1 (**Fig. 13**). The carboxylate group on the inhibitors LHS probably binds in the same orientation to CysK1 as to CysM, based on the conserved active-site residues binding the carboxylate group on all so far identified L-cysteine synthase inhibitors. The RHS, however, is very unlikely to bind in the

same fashion in CysK1 as observed in CysM, because this orientation would result in severe clashes between inhibitor and a loop segment, stretching from P217 to G224.

3.3.4 Targeting all three L-cysteine synthases at once

Although the three L-cysteine synthases are active during different metabolic states, it would be of great importance to inhibit all three L-cysteine synthases at once. The three pathways are redundant and could potentially provide back-up systems for each other, taking over L-cysteine production upon specific inhibition of only one of the three L-cysteine synthases and thus leading to drug resistance. By inhibiting all three L-cysteine synthases at once, the onset of drug resistance caused by the redundancy of L-cysteine synthases could potentially be postponed.

3.4 CONCLUSION

In **paper I**, CysC, the APS kinase domain of mycobacterial ATP sulfurylase was characterized in a mechanistic and structural manner. The study further identified an L-cysteine residue that controls lid dynamics important for catalytic activity. The overall structure of the human homologs PAPSS1 and PAPSS2 and the mycobacterial CysC are very similar and so are the substrate binding sites, which share a significant degree of sequence identity.

Paper II describes the successful identification of inhibitors targeting CysM, the L-cysteine synthase most active during dormancy. Seven compounds have been identified that bind in the active site of CysM with affinities clustering in the low micromolar range. These compounds also inhibit the enzyme, and the high resolution structures of the protein ligand complexes in combination with the inhibition data from the set of 71 compounds designed and selected by systematic ligand expansion allows for description of SAR. Four of the identified inhibitors were shown to outperform currently used antibiotics in terms of killing non-replicating *Mtb* shown in a nutrient starvation model.

In **paper III**, it was shown that inhibitors targeting CysM also show inhibitory power against CysK1 and CysK2. Superposition of the complex structures of CysK1 and thiazolidine and CysM and compound **2** underpin the hypothesis that the carboxylate group on the LHS of the urea-based compounds bind in the same cleft in CysK1 as the carboxylate group of the thiazolidine inhibitor does. The RHS of the urea-based inhibitors however is unlikely to bind in the same orientation as observed in CysM, because this would result in severe clashes with CysK1.

In conclusion, developing specific inhibitors targeting only the mycobacterial CysC, without targeting human homologs, seems very challenging, due to a high degree of similarity between the enzymes of the two species, as has been shown in paper I. The identified inhibitors targeting CysM, CysK1 and CysK2 in paper II and III however could provide a valuable starting point to develop a drug that inhibits all three L-cysteine synthases at once.

4 ACKNOWLEDGEMENTS

I started a Ph.D. because I had the feeling that so many questions were unanswered. Now, almost six years later, I am not sure if I got the answers I was looking for or if I have more questions than I have ever had before. I am very grateful for this time that not only taught me science, but also taught me a lot about myself and shaped me as a person.

I would like to thank my main supervisor **Gunter**, for giving me the possibility to perform my doctoral studies at MSB. Thank you for your scientific input, your guidance and support through the meanders of biochemistry and biophysics. Although there is a long way ahead, I know you prepared me well for upcoming scientific challenges. I think one of the most important things you taught me is never to lose your principles, no matter how tempting the reward might be. Mit Wehmut verabschiede ich mich, ich bin aus dem Schneider.

Robi, I am not sure if any other Ph.D. student was forced to learn as many methods as I was. It was amazing what you taught me and I cannot thank you enough for this toolbox. I never made a secret out of the fact that you truly became the uncle I never had. The reasons are manifold and the list is too long to be written, but I need to make some things clear before I go for good, once and for all so that you never forget. Listen to the end! And no Robi, Deep Purple did not have their peak time when David Coverdale was their singer! Miss you already and I hope you catch the real big fish, in whatever sense.

Thank you, **Bernie**, for being a bit of an off-the-record supervisor. I appreciate all the Coot tricks that I could scavenge from you and that you often tried to challenge me during our seminars. There should definitely be more of your kind. I am utterly sad that I never had the chance to join the Mars mission team.

My evaste **Eva**, it is very sad that our time as fellow Ph.D. students is now coming to an end. Through blood, sweat and sometimes close to tears, mostly because of laughter, I made some of the best memories of my life in your presence. If we only would have recorded the 24 hours before your wedding, we would be rich by now.

Thank you to all the present and past **members of MSB** that I now can call friends in all parts of the world. It was a pleasure to work and laugh with you. In particular, I want to thank you, **Ahmad** for being the helping hand in the lab and for making sure that we never drowned in our own mess. **Dominic**, even though you are so far away now, I want to thank you for teaching me the necessary skills to survive in a research group at KI. I miss you quite many times. I also want to mention the **PSF** gang, **Helena**, **Tomas**, **Martin**, **Ida** and **Ruairi**, without you, most of the experiments would not be possible, thank you for teaching, expressing and lending! Thank you to all the other scientists that I have had the pleasure of meeting and collaborating with.
One more person that should not be missing here, **Erika**, you have been a mentor for me from when I was a Bachelor student, thank you for always taking your time, when I spontaneously crashed your office.

Dominik, you are definitely among my favorite people, with the best taste in music, I thought at least until the last Friday in March 2017. I know, I neglected our weekly meetings lately, but this is no excuse to ever listen to Eros and enjoy it. I cannot even properly acknowledge you. Dr. **Juha**, my private dancer and medical advisor, I am glad you do not fit into a drawer and I assure you, you will never have a more entertaining patient than me. **Maria**, it feels like ages ago that we sat in the same office and got make-up cake, what a journey from then to now, thank you for being part of it.

Irina, I have to say, I did not miss stastics (for all the others, this is not a typo) too much, but sometimes coffee or ice cream with you would be more than nice. Hamburg is calling me. **Rozbeh**, I think your mother will move on now and no, she is not paying allowance. **Essam**, without you the acknowledgements would be much shorter. Thank you for integrating me into the social life of KI and so much more. **Will**, you truly raised the level on the trashy scale to 22. **Olle**, thank you for the coffee! **Håkan**, my favorite dandy, you still owe Laura and me margaritas, we put it on ice for now, but we won't forget. **Francesca**, my complaints department, thank you for always being on my side. **Andrea**, you have no idea how many lives cow foot has saved so far.

Gottfrank, leider war deine Zeit um, bevor ich dir dieses Buch überreichen konnte. Danke, für deinen tiefen Respekt, für den Weg, den ich gewählt habe. Du bist immer bei mir, in Gedanken, in meiner Sturheit und meinem Durchhaltevermögen. **Doris**, die Tänzerin im Sturm. Thank you for your unshakeable belief in me. You always motivated me and inspired me to accept new challenges and to never give up. Without you, I would not be where I am now. **Gyross**, you are the best second mum on this planet and you were so damn right, when you said, "If you are riding a dead horse, jump off and absolutely do not try to put two dead horses together if you want to get any further" and thank you that the Cava pipeline never ran dry. My dear **RoBru Sistaz**, it feels very safe knowing that there is a place to come home to that is always filled with joy and laughter. Danke, dass du den Forschergeist in mir geweckt hast, **Papa**, und mich trotzdem jedes Mal wieder zum Wundern bringst, wenn das rationale Denken überhand nimmt.

There are people that fall from the sky and become so fundamental that one ends up in joining them in the most meaningful quest of their lives. One is allowed to witness an event that turns everything upside down and suddenly everything starts to make sense. Thank you for your trust, **Shiromi**! **Sanja**, my rock, with you at my side, I will never lose a war. We started this Nordic journey together and it feels strange that it soon might come to an end. I would go to the end of the world with you, but only with hallonsaft and falafel.

Laurent, even though we are hardly ever of the same opinion, I enjoy our discussions so much. They are always deeply meaningful and always create something novel. **Christine**, I would have never thought that there are people on this planet that understand without explanation, without judgement. Unexpected that two windows open at the same time can result in something so precious. To more Cava, more songs and more concerts. **Laura**, you are the only one with whom I would ever hitchhike again. I really felt like Alice falling into

the rabbit hole while meeting the king of Ha-Ha. When I think about it, I went through the most dangerous situations of my life with you. For now, to more songs and more concerts.

Tina, it is a pity that we cannot sit on each other's balconies spontaneously. I miss you very often, especially when I do stupid things. I always would want to tell you in person and read in your face what you think. Thank you for being one of my most truthful companions. **Babsi**, Russian ball pit is only awesome in your presence, maybe tigers and pigeons would double the fun. **Anta**, we need to go to Porto. Can we please finally bring all the unicorns together and start riding towards the West. It is really about time, I miss the laughter. **Dita**, I always feel like a child when we go for new adventures. I am glad that strawberry yoghurt still does not have any fish bones. Thank you for being my biggest fan and for pushing the creative half of me. **Markus**, it is a pity that our travel plans did not match this time, but I insist we give it at least one more try.

Dorian Stain, I am very grateful that you unleash the creativity from deep within.

5 REFERENCES

Akira, S., Uematsu, S. et al. (2006). "Pathogen Recognition and Innate Immunity." Cell **124**(4):783-801.

Alnimr, A. M. (2015). "Dormancy models for *Mycobacterium tuberculosis*: A minireview." Brazilian Journal of Microbiology **46**(3):641-647.

Amori, L., Katkevica, S. et al. (2012). "Design and synthesis of trans-2-substituted-cyclopropane-1-carboxylic acids as the first non-natural small molecule inhibitors of O-acetylserine sulfhydrylase." Medicinal Chemical Communications **3**(9):1111-1116.

Andries, K., Verhasselt, P. et al. (2005). "A Diarylquinoline Drug Active on the ATP Synthase of *Mycobacterium tuberculosis*." Science **307**(5707):223-227.

Armstrong, J. A. & Hart P. D. A. (1971). "Response of cultured macrophages to *Mycobacterium tuberculosis*, with observations on fusion of lysosomes with phagosomes." The Journal of Experimental Medicine **134**(3):713-740.

Awuh, J. A. & Flo T. H. (2016). "Molecular basis of mycobacterial survival in macrophages." Cellular and Molecular Life Sciences:1-24.

Baker, O., Lee, O. Y. C. et al. (2015). "Human tuberculosis predates domestication in ancient Syria." Tuberculosis **95, Supplement 1**:S4-S12.

Betts, J. C., Lukey, P. T. et al. (2002). "Evaluation of a nutrient starvation model of *Mycobacterium tuberculosis* persistence by gene and protein expression profiling." Molecular Microbiology **43**(3):717-731.

Bhave, D. P., Hong, J. A. et al. (2011). "Spectroscopic Studies on the [4Fe-4S] Cluster in Adenosine 5′-Phosphosulfate Reductase from *Mycobacterium tuberculosis*." The Journal of Biological Chemistry **286**(2):1216-1226.

Bhave, D. P., Muse, W. B. et al. (2007). "Drug Targets in Mycobacterial Sulfur Metabolism." Infectious disorders drug targets **7**(2):140-158.

Bleicher, K. H., Bohm, H. J. et al. (2003). "Hit and lead generation: beyond high-throughput screening." Nature Reviews Drug Discovery **2**(5):369-378.

Blondiaux, N., Moune, M. et al. (2017). "Reversion of antibiotic resistance in *Mycobacterium tuberculosis* by spiroisoxazoline SMARt-420." Science **355**(6330):1206-1211.

Bonner, E. R., Cahoon, R. E. et al. (2005). "Molecular basis of cysteine biosynthesis in plants: structural and functional analysis of O-acetylserine sulfhydrylase from *Arabidopsis thaliana*." Journal of Biological Chemistry **280**(46):38803-38813.

Bornemann, C., Jardine, M. A. et al. (1997). "Biosynthesis of mycothiol: elucidation of the sequence of steps in *Mycobacterium smegmatis*." Biochemical Journal **325**(Pt 3):623-629.

Burns, K. E., Baumgart, S. et al. (2005). "Reconstitution of a new Cysteine biosynthetic pathway in *Mycobacterium tuberculosis*." Journal of the American Chemical Society **127**(33):11602-11603.

Calmette, A. (1922). "L'infection bacillaire et la tuberculose chez l'homme et chez les animaux processus d'infection, et de defense, étude biologique et expérimentale." from http://books.google.com/books?id=PBk1AQAAMAAJ, accessed 15th of March, 2017.

Cambau, E. & Drancourt M. (2014). "Steps towards the discovery of *Mycobacterium tuberculosis* by Robert Koch, 1882." Clinical Microbiology and Infection **20**(3):196-201.

Campanini, B., Benoni, R. et al. (2015). "Moonlighting O-acetylserine sulfhydrylase: New functions for an old protein." Biochimica et biophysica acta **1854**(9):1184-1193.

Campanini, B., Speroni, F. et al. (2005). "Interaction of serine acetyltransferase with O-acetylserine sulfhydrylase active site: Evidence from fluorescence spectroscopy." Protein Science **14**(8):2115-2124.

Carroll, K. S., Gao, H. et al. (2005). "A Conserved Mechanism for Sulfonucleotide Reduction." PLOS Biology **3**(8):e250.

Chai, C. L. L. & Mátyus, P. (2015). "One size does not fit all: Challenging some dogmas and taboos in drug discovery." Future Medicinal Chemistry **8**(1):29-38.

Cole, S. T., Brosch, R. et al. (1998). "Deciphering the biology of *Mycobacterium tuberculosis* from the complete genome sequence." Nature **393**(6685):537-544.

Comas, I., Coscolla, M. et al. (2013). "Out-of-Africa migration and Neolithic coexpansion of *Mycobacterium tuberculosis* with modern humans." Nature Genetics **45**(10):1176-1182.

Comas, I. & Gagneux, S. (2009). "The Past and Future of Tuberculosis Research." PLoS Pathogens **5**(10):e1000600.

Copenhaver, R. H., Sepulveda, E. et al. (2004). "A Mutant of *Mycobacterium tuberculosis* H37Rv That Lacks Expression of Antigen 85A Is Attenuated in Mice but Retains Vaccinogenic Potential." Infection and Immunity **72**(12):7084-7095.

Cox, E. & Laessig, K. (2014). "FDA Approval of Bedaquiline — The Benefit–Risk Balance for Drug-Resistant Tuberculosis." New England Journal of Medicine **371**(8):689-691.

Cunningham-Bussel, A., Zhang, T. et al. (2013). "Nitrite produced by *Mycobacterium tuberculosis* in human macrophages in physiologic oxygen impacts bacterial ATP consumption and gene expression." Proceedings of the National Academy of Sciences of the United States of America **110**(45):E4256-E4265.

Davis, J. M. & Ramakrishnan L. (2008). "“The Very Pulse of the Machine”: The Tuberculous Granuloma in Motion." Immunity **28**(2):146-148.

Davis, J. M. & Ramakrishnan L. (2009). "The Role of the Granuloma in Expansion and Dissemination of Early Tuberculous Infection." Cell **136**(1):37-49.

Diacon, A. H., Pym, A. et al. (2014). "Multidrug-Resistant Tuberculosis and Culture Conversion with Bedaquiline." New England Journal of Medicine **371**(8):723-732.

Diamond, J. M. (1999). “Guns, Germs, and Steel: The Fates of Human Societies.” New York: W. W. Norton & Company.

Ehrt, S. & Schnappinger D. (2009). "Mycobacterial survival strategies in the phagosome: Defense against host stresses." Cellular microbiology **11**(8):1170-1178.

Ernst, J. D. (2012). "The immunological life cycle of tuberculosis." Nature Reviews Immunology **12**(8):581-591.

Fan, F., Vetting, M. W. et al. (2009). "Structures and Mechanisms of the Mycothiol Biosynthetic Enzymes." Current opinion in chemical biology **13**(4):444-452.

Fitzgerald, D. W., Sterling, T. R. et al. (2015). "*Mycobacterium tuberculosis*" In Mandell, Douglas, and Bennett's Principles and Practice of Infectious Diseases (pp. 2787-2818) Philadelphia: ELSEVIER.

Fogel, N. (2015). "Tuberculosis: A disease without boundaries." Tuberculosis **95**(5):527-531.

Fuda, H., Shimizu, C. et al. (2002). "Characterization and expression of human bifunctional 3'-phosphoadenosine 5'-phosphosulphate synthase isoforms." Biochemical Journal **365**(Pt 2):497-504.

Gaitonde, M. K. (1967). "A spectrophotometric method for the direct determination of cysteine in the presence of other naturally occurring amino acids." Biochemical Journal **104**(2):627-633.

Gay, S. C., Segel, I. H. et al. (2009). "Structure of the two-domain hexameric APS kinase from *Thiobacillus denitrificans*: structural basis for the absence of ATP sulfurylase activity." Acta Crystallographica Section D: Biological Crystallography **65**(Pt 10):1021-1031.

Gengenbacher, M. & Kaufmann, S. H. E. (2012). "*Mycobacterium tuberculosis*: success through dormancy." FEMS Microbiology Reviews **36**(3):514-532.

Gilleron, M., Stenger, S. et al. (2004). "Diacylated Sulfoglycolipids Are Novel Mycobacterial Antigens Stimulating CD1-restricted T Cells during Infection with *Mycobacterium tuberculosis*." The Journal of Experimental Medicine **199**(5):649-659.

Gilmore, S. A., Schelle, M. W. et al. (2012). "Sulfolipid-1 Biosynthesis Restricts *Mycobacterium tuberculosis* Growth in Human Macrophages." ACS Chemical Biology **7**(5):863-870.

Goren, M. B., Brokl, O. et al. (1974). "Lipids of Putative Relevance to Virulence in *Mycobacterium tuberculosis*: Correlation of Virulence with Elaboration of Sulfatides and Strongly Acidic Lipids." Infection and Immunity **9**(1):142-149.

Gotor, C. & Romero, L. C. (2013). "S-sulfocysteine synthase function in sensing chloroplast redox status." Plant Signaling & Behavior **8**(3):e23313.

Halkier, B. A. & Gershenzon, J. (2006). "Biology and biochemistry of glucosinulates." Annual Review of Plant Biology **57**(1):303-333.

Hampshire, T., Soneji, S. et al. (2004). "Stationary phase gene expression of *Mycobacterium tuberculosis* following a progressive nutrient depletion: a model for persistent organisms?" Tuberculosis (Edinburgh, Scotland) **84**(3-4):228-238.

Harjes, S., Bayer, P. et al. (2005). "The Crystal Structure of Human PAPS Synthetase 1 Reveals Asymmetry in Substrate Binding." Journal of Molecular Biology **347**(3):623-635.

Hatherill, M., Tait, D. et al. (2016). "Clinical Testing of Tuberculosis Vaccine Candidates." Microbiology Spectrum **4**(5):1-18.

Hatzios, S. K., Iavarone, A. T. et al. (2008). "Rv2131c from *Mycobacterium tuberculosis* Is a CysQ 3′-Phosphoadenosine-5′-phosphatase." Biochemistry **47**(21):5823-5831.

Hatzios, S. K., Schelle, M. W. et al. (2011). "The *Mycobacterium tuberculosis* CysQ phosphatase modulates the biosynthesis of sulfated glycolipids and bacterial growth." Bioorganic & medicinal chemistry letters **21**(17):4956-4959.

Hell R. D., Knaff, C. et al. (2008). Sulfur Metabolism in Phototrophic Organisms. **249 Supplement 2**:S147-55.

Henzler-Wildman, K. & Kern D. (2007). "Dynamic personalities of proteins." Nature **450**(7172):964-972.

Herrmann, J., Nathin, D. et al. (2015). "Recapitulating the Structural Evolution of Redox Regulation in Adenosine 5′-Phosphosulfate Kinase from Cyanobacteria to Plants." The Journal of Biological Chemistry **290**(41):24705-24714.

Hershberg, R., Lipatov, M. et al. (2008). "High Functional Diversity in *Mycobacterium tuberculosis* Driven by Genetic Drift and Human Demography." PLOS Biology **6**(12):e311.

Hopewell, P. C., Kato-Maeda, M. et al. (2016). "Tuberculosis." In Murray and Nadel's Textbook of Respiratory Medicine. (pp. 593-628) Philadelphia: ELSEVIER.

Horsburgh, C. R., Barry, C. E. et al. (2015). "Treatment of Tuberculosis." New England Journal of Medicine **373**(22):2149-2160.

Huang, B., Vetting, M. W. et al. (2005). "The Active Site of O-Acetylserine Sulfhydrylase Is the Anchor Point for Bienzyme Complex Formation with Serine Acetyltransferase." Journal of Bacteriology **187**(9):3201-3205.

Hughes, J. P., Rees, S. et al. (2011). "Principles of early drug discovery." British Journal of Pharmacology **162**(6):1239-1249.

Hussell, T. & Bell, T. J. (2014). "Alveolar macrophages: plasticity in a tissue-specific context." Nat Rev Immunol **14**(2):81-93.

Jothivasan, V. K. & Hamilton, C. J. (2008). "Mycothiol: synthesis, biosynthesis and biological functions of the major low molecular weight thiol in actinomycetes." Natural Product Reports **25**(6):1091-1117.

Jurgenson, C. T., Burns, K. E. et al. (2008). "Crystal Structure of a Sulfur Carrier Protein Complex Found in the Cysteine Biosynthetic Pathway of *Mycobacterium tuberculosis*." Biochemistry **47**(39):10354-10364.

Keshavjee, S. & Farmer, P. E. (2012). "Tuberculosis, Drug Resistance, and the History of Modern Medicine." New England Journal of Medicine **367**(10):931-936.

Koch, R. (1882). "Die Aetiologie der Tuberkulose" Berliner klinische Wochenschrift **15**:221–230.

Kredich, N. M. M., Hulanicka, D. et al. (1979). "Synthesis of L-cysteine in *Salmonella typhimurium*." Ciba Found Symp **72**:87-99.

Kremer, K., Glynn, J. R. et al. (2004). "Definition of the Beijing/W Lineage of *Mycobacterium tuberculosis* on the Basis of Genetic Markers." Journal of Clinical Microbiology **42**(9):4040-4049.

Kumar, A., Toledo, J. C. et al. (2007). "*Mycobacterium tuberculosis* DosS is a redox sensor and DosT is a hypoxia sensor." Proceedings of the National Academy of Sciences of the United States of America **104**(28):11568-11573.

Kuznetsova, S., Knaff, D. B. et al. (2004). "Mechanism of Spinach Chloroplast Ferredoxin-Dependent Nitrite Reductase: Spectroscopic Evidence for Intermediate States." Biochemistry **43**(2):510-517.

Lansdon, E. B., Fisher, A. J. et al. (2004). "Human 3‘-Phosphoadenosine 5‘-Phosphosulfate Synthetase (Isoform 1, Brain): Kinetic Properties of the Adenosine Triphosphate Sulfurylase and Adenosine 5‘-Phosphosulfate Kinase Domains." Biochemistry **43**(14):4356-4365.

Lawn, S. D. & Zumla, A. I. (2011). "Tuberculosis." The Lancet **378**(9785):57-72.

Lay, G., Poquet, Y. et al. (2007). "Langhans giant cells from *M. tuberculosis*-induced human granulomas cannot mediate mycobacterial uptake." The Journal of Pathology **211**(1):76-85.

Lee, W., VanderVen, B. C. et al. (2013). "Intracellular *Mycobacterium tuberculosis* Exploits Host-derived Fatty Acids to Limit Metabolic Stress." The Journal of Biological Chemistry **288**(10):6788-6800.

Leipe, D. D., Koonin, E. V. et al. (2003). "Evolution and Classification of P-loop Kinases and Related Proteins." Journal of Molecular Biology **333**(4):781-815.

Leistikow, R. L., Morton, R. A. et al. (2010). "The *Mycobacterium tuberculosis* DosR Regulon Assists in Metabolic Homeostasis and Enables Rapid Recovery from Nonrespiring Dormancy." Journal of Bacteriology **192**(6):1662-1670.

Lenaerts, A., Barry, C. E. et al. (2015). "Heterogeneity in tuberculosis pathology, microenvironments and therapeutic responses." Immunological Reviews **264**(1):288-307.

Lillig, C. H., Schiffmann, S. et al. (2001). "Molecular and Catalytic Properties of *Arabidopsis thaliana* Adenylyl Sulfate (APS)-Kinase." Archives of Biochemistry and Biophysics **392**(2):303-310.

Lipinski, C. A., Lombardo, F. et al. (2001). "Experimental and computational approaches to estimate solubility and permeability in drug discovery and development settings1." Advanced Drug Delivery Reviews **46**(1–3):3-26.

Luca, S. & Mihaescu T. (2013). "History of BCG Vaccine." Mædica **8**(1):53-58.

Mack, U., Migliori, G. B. et al. (2009). "LTBI: latent tuberculosis infection or lasting immune responses to M. tuberculosis? A TBNET consensus statement." European Respiratory Journal **33**(5):956-973.

MacRae, I. J., Segel, I. H. et al. (2000). "Crystal Structure of Adenosine 5‘-Phosphosulfate Kinase from *Penicillium chrysogenum*." Biochemistry **39**(7):1613-1621.

Malojčić, G., Owen, R. L. et al. (2014). "Structural and Mechanistic Insights into the PAPS-Independent Sulfotransfer Catalyzed by Bacterial Aryl Sulfotransferase and the Role of the DsbL/DsbI System in Its Folding." Biochemistry **53**(11):1870-1877.

Martin, C. J., Carey, A. F. et al. (2016). "A bug’s life in the granuloma." Seminars in immunopathology **38**(2):213-220.

Martinez, F. O. & Gordon, S. (2014). "The M1 and M2 paradigm of macrophage activation: time for reassessment." F1000Prime Reports **6**:1-13.

Mayer-Barber, K. D., Andrade, B. B. et al. (2011). "Innate and adaptive interferons suppress IL-1α and IL-1β production by distinct pulmonary myeloid subsets during *Mycobacterium tuberculosis* infection." Immunity **35**(6):1023-1034.

Merker, M., Blin, C. et al. (2015). "Evolutionary history and global spread of the *Mycobacterium tuberculosis* Beijing lineage." Nature Genetics **47**(3):242-249.

Mikušová, K. & Ekins, S. (2017). "Learning from the past for TB drug discovery in the future." Drug Discovery Today **22**(3):534-545.

Mosser, D. M. & Edwards, J. P. (2008). "Exploring the full spectrum of macrophage activation." Nature Reviews Immunology **8**(12):958-969.

Mougous, J. D., Green, R. E. et al. (2002). "Sulfotransferases and Sulfatases in Mycobacteria." Chemistry & Biology **9**(7):767-776.

Mugford, S. G., Matthewman, C. A. et al. (2010). "Adenosine-5′-phosphosulfate kinase is essential for Arabidopsis viability." FEBS Letters **584**(1):119-123.

Nakatani, T., Ohtsu, I. et al. (2012). "Enhancement of thioredoxin/glutaredoxin-mediated L-cysteine synthesis from S-sulfocysteine increases L-cysteine production in *Escherichia coli*." Microbial Cell Factories **11**:62-62.

Nambi, S., Long, J. E. et al. (2015). "The oxidative stress network of *Mycobacterium tuberculosis* reveals coordination between radical detoxification systems." Cell host & microbe **17**(6):829-837.

Niederweis, M. (2008). "Nutrient acquisition by mycobacteria." Microbiology **154**(3):679-692.

Novikov, A., Cardone, M. et al. (2011). "*Mycobacterium tuberculosis* triggers host type I interferon signaling to regulate IL-1β production in human macrophages." Journal of immunology **187**(5):2540-2547.

O'Leary, S. E., Jurgenson, C. T. et al. (2008). "O-Phospho-L-serine and the Thiocarboxylated Sulfur Carrier Protein CysO-COSH are Substrates for CysM, a Cysteine Synthase from *Mycobacterium tuberculosis*." Biochemistry **47**(44):11606-11615.

Palde, P. B., Bhaskar, A. et al. (2016). "First-in-Class Inhibitors of Sulfur Metabolism with Bactericidal Activity against Non-Replicating M. tuberculosis." ACS Chemical Biology **11**(1):172-184.

Pandey, A. K. & Sassetti, C. M. (2008). "Mycobacterial persistence requires the utilization of host cholesterol." Proceedings of the National Academy of Sciences of the United States of America **105**(11):4376-4380.

Peyron, P., Vaubourgeix, J. et al. (2008). "Foamy Macrophages from Tuberculous Patients' Granulomas Constitute a Nutrient-Rich Reservoir for M. tuberculosis Persistence." PLoS Pathogens **4**(11):e1000204.

Philips, J. A. & Ernst, J. D. (2012). "Tuberculosis Pathogenesis and Immunity." Annual Review of Pathology: Mechanisms of Disease **7**(1):353-384.

Pi, N., Hoang, M. B. et al. (2005). "Kinetic measurements and mechanism determination of Stf0 sulfotransferase using mass spectrometry." Analytical Biochemistry **341**(1):94-104.

Pieroni, M., Annunziato, G. et al. (2016). "Rational Design, Synthesis, and Preliminary Structure–Activity Relationships of α-Substituted-2-Phenylcyclopropane Carboxylic Acids as Inhibitors of *Salmonella typhimurium* O-Acetylserine Sulfhydrylase." Journal of Medicinal Chemistry **59**(6):2567-2578.

Pinto, R., Harrison, J. S. et al. (2007). "Sulfite Reduction in Mycobacteria." Journal of Bacteriology **189**(18):6714-6722.

Poyraz, Ö., Brunner, K. et al. (2015). "Crystal Structures of the Kinase Domain of the Sulfate-Activating Complex in *Mycobacterium tuberculosis*." PLOS ONE **10**(3):e0121494.

Poyraz, Ö., Jeankumar, V. U. et al. (2013). "Structure-Guided Design of Novel Thiazolidine Inhibitors of O-Acetyl Serine Sulfhydrylase from *Mycobacterium tuberculosis*." Journal of medicinal chemistry **56**(16):6457-6466.

Puissegur, M.-P., Lay, G. et al. (2007). "Mycobacterial Lipomannan Induces Granuloma Macrophage Fusion via a TLR2-Dependent, ADAM9- and β1 Integrin-Mediated Pathway." The Journal of Immunology **178**(5):3161-3169.

Rabeh, W. M. & Cook, P. F. (2004). "Structure and Mechanism of O-Acetylserine Sulfhydrylase." Journal of Biological Chemistry **279**(26):26803-26806.

Raj, I., Mazumder, M. et al. (2013). "Molecular basis of ligand recognition by OASS from *E. histolytica*: Insights from structural and molecular dynamics simulation studies." Biochimica et Biophysica Acta (BBA) - General Subjects **1830**(10):4573-4583.

Ravilious, G. E. & Jez, J. M. (2012). "Nucleotide Binding Site Communication in *Arabidopsis thaliana* Adenosine 5′-Phosphosulfate Kinase." The Journal of Biological Chemistry **287**(36):30385-30394.

Ravilious, G. E. & Jez, J. M. (2012). "Structural biology of plant sulfur metabolism: From assimilation to biosynthesis." Natural Product Reports **29**(10):1138-1152.

Rege, V. D., Kredich, N. M. et al. (1996). "A Change in the Internal Aldimine Lysine (K42) in O-Acetylserine Sulfhydrylase to Alanine Indicates Its Importance in Transimination and as a General Base Catalyst." Biochemistry **35**(41):13485-13493.

Rengarajan, J., Bloom, B. R. et al. (2005). "Genome-wide requirements for *Mycobacterium tuberculosis* adaptation and survival in macrophages." Proceedings of the National Academy of Sciences of the United States of America **102**(23):8327-8332.

Renosto, F., Seubert, P. A. et al. (1984). "Adenosine 5'-phosphosulfate kinase from *Penicillium chrysogenum*. Purification and kinetic characterization." Journal of Biological Chemistry **259**(4):2113-2123.

Rivera-Marrero, C. A., Ritzenthaler, J. D. et al. (2002). "Molecular cloning and expression of a novel glycolipid sulfotransferase in *Mycobacterium tuberculosis*." Microbiology **148**(3):783-792.

Rufai, S. B., Sankar, M. M. et al. (2016). "Predominance of Beijing lineage among pre-extensively drug-resistant and extensively drug-resistant strains of *Mycobacterium tuberculosis*: A tertiary care center experience." International Journal of Mycobacteriology **5, Supplement 1**:S197-S198.

Salgame, P., Geadas, C. et al. (2015). "Latent tuberculosis infection – Revisiting and revising concepts." Tuberculosis **95**(4):373-384.

Salsi, E., Bayden, A. S. et al. (2010). "Design of O-acetylserine sulfhydrylase inhibitors by mimicking Nature." Journal of medicinal chemistry **53**(1):345-356.

Sassetti, C. M. & Rubin, E. J. (2003). "Genetic requirements for mycobacterial survival during infection." Proceedings of the National Academy of Sciences of the United States of America **100**(22):12989-12994.

Satishchandran, C., Hickman, Y. et al. (1992). "Characterization of the phosphorylated enzyme intermediate formed in the adenosine 5'-phosphosulfatekinase reaction." Biochemistry **31**(47):11684-11688.

Satishchandran, C. & Markham, G. D. (1989). "Adenosine-5'-phosphosulfate kinase from *Escherichia coli* K12. Purification, characterization, and identification of a phosphorylated enzyme intermediate." Journal of Biological Chemistry **264**(25):15012-15021.

Satishchandran, C. & Markham, G. D. (2000). "Mechanistic Studies of *Escherichia coli* Adenosine-5′-phosphosulfate Kinase." Archives of Biochemistry and Biophysics **378**(2):210-215.

Schaible, U. E., Sturgill-Koszycki, S. et al. (1998). "Cytokine Activation Leads to Acidification and Increases Maturation of *Mycobacterium avium*-Containing Phagosomes in Murine Macrophages." The Journal of Immunology **160**(3):1290-1296.

Schelle, M. W. & Bertozzi, C. R. (2006). "Sulfate Metabolism in Mycobacteria." ChemBioChem **7**(10):1516-1524.

Schnappinger, D., Ehrt, S. et al. (2003). "Transcriptional Adaptation of *Mycobacterium tuberculosis* within Macrophages: Insights into the Phagosomal Environment." The Journal of Experimental Medicine **198**(5):693-704.

Schneider, G., Käck, H. et al. (2000). "The manifold of vitamin B6 dependent enzymes." Structure **8**(1):R1-R6.

Schnell, R., Oehlmann, W. et al. (2007). "Structural insights into catalysis and inhibition of O-acetylserine sulfhydrylase from *Mycobacterium tuberculosis*. Crystal structures of the enzyme alpha-aminoacrylate intermediate and an enzyme-inhibitor complex." The Journal of biological chemistry **282**(32):23473-23481.

Schnell, R., Sandalova, T. et al. (2005). "Siroheme- and [Fe4-S4]-dependent NirA from *Mycobacterium tuberculosis* Is a Sulfite Reductase with a Covalent Cys-Tyr Bond in the Active Site." Journal of Biological Chemistry **280**(29):27319-27328.

Schnell, R., Sriram, D. et al. (2015). "Pyridoxal-phosphate dependent mycobacterial cysteine synthases: Structure, mechanism and potential as drug targets." Biochimica et biophysica acta **1854**(9):1175-1183.

Schulz, G., Elzinga, M. et al. (1974). "Three dimensional structure of adenyl kinase." Nature **250**(462):120-123.

Sekowska, A., Kung, H.-F. et al. (2000). "Sulfur metabolism in *Escherichia coli* and related bacteria: facts and fiction." Journal of Molecular Microbiology and Biotechnology **2**(2):145-177.

Sekulic, N., Konrad, M. et al. (2007). "Structural Mechanism for Substrate Inhibition of the Adenosine 5′-Phosphosulfate Kinase Domain of Human 3′-Phosphoadenosine 5′-Phosphosulfate Synthetase 1 and Its Ramifications for Enzyme Regulation." Journal of Biological Chemistry **282**(30):22112-22121.

Singh, B. & Schwartz, N. B. (2003). "Identification and Functional Characterization of the Novel BM-motif in the Murine Phosphoadenosine Phosphosulfate (PAPS) Synthetase." Journal of Biological Chemistry **278**(1):71-75.

Smith, T., Wolff, K. A. et al. (2013). "Molecular Biology of Drug Resistance in *Mycobacterium tuberculosis*." Current topics in microbiology and immunology **374**:53-80.

Spigelman, M., Donoghue, H. D. et al. "Evolutionary changes in the genome of *Mycobacterium tuberculosis* and the human genome from 9000 years BP until modern times." Tuberculosis **95**:S145-S149.

Steiner, E. M., Böth, D. et al. (2014). "CysK2 from *Mycobacterium tuberculosis* is an O-phospho-L-serine-dependent S-sulfocysteine synthase." Journal of bacteriology **196**(19):3410-3420.

Stipanuk, M. H. (2004). "Sulfur amino acid metabolism: Pathways for Production and Removal of Homocysteine and Cysteine." Annual Review of Nutrition **24**(1):539-577.

Sun, M., Andreassi, J. L. et al. (2005). "The Trifunctional Sulfate-activating Complex (SAC) of *Mycobacterium tuberculosis*." Journal of Biological Chemistry **280**(9):7861-7866.

Swinney, D. C. & Anthony, J. (2011). "How were new medicines discovered?" Nature Reviews Drug Discovery **10**(7):507-519.

Takahashi H. K. S., Giordano M. Et al. (2011). "Sulfur Assimilation in Photosynthetic Organisms: Molecular Functions and Regulations of Transporters and Assimilatory Enzymes." Annual Review of Plant Biology **62**(1):157-184.

Wallis, R. S., Maeurer, M. et al. (2016). "Tuberculosis—advances in development of new drugs, treatment regimens, host-directed therapies, and biomarkers." The Lancet Infectious Diseases **16**(4):e34-e46.

Weiss, G. & Schaible, U. E. (2015). "Macrophage defense mechanisms against intracellular bacteria." Immunological Reviews **264**(1):182-203.

Venkatachalam, K. V. (2003). "Human 3'-phosphoadenosine 5'-phosphosulfate (PAPS) Synthase: Biochemistry, Molecular Biology and Genetic Deficiency." IUBMB Life **55**(1):1-11.

Via, L. E., Lin, P. L. et al. (2008). "Tuberculous Granulomas Are Hypoxic in Guinea Pigs, Rabbits, and Nonhuman Primates." Infection and Immunity **76**(6):2333-2340.

Williams, S. J., Senaratne, R. H. et al. (2002). "5′-Adenosinephosphosulfate Lies at a Metabolic Branch Point in *Mycobacteria*." Journal of Biological Chemistry **277**(36):32606-32615.

Wilson, L. G. (2004). "Commentary: Medicine, population, and tuberculosis." International Journal of Epidemiology **34**(3):521-524.

Wolf-Watz, M., Thai, V. et al. (2004). "Linkage between dynamics and catalysis in a thermophilic-mesophilic enzyme pair." Nature Structural & Molecular Biology **11**(10):945-949.

Wolschendorf, F., Mahfoud, M. et al. (2007). "Porins Are Required for Uptake of Phosphates by *Mycobacterium smegmatis*." Journal of Bacteriology **189**(6):2435-2442.

Wooff, E., Michell, S. L. et al. (2002). "Functional genomics reveals the sole sulphate transporter of the *Mycobacterium tuberculosis* complex and its relevance to the acquisition of sulphur *in vivo*." Molecular Microbiology **43**(3):653-663.

World Health Organization (2016). "Global tuberculosis report." from http://www.who.int/tb/publications/global_report/en/, accessed 25th March 2017.

Voskuil, M. I., Bartek, I. L. et al. (2011). "The Response of *Mycobacterium tuberculosis* to Reactive Oxygen and Nitrogen Species." Frontiers in Microbiology **2**:105.

Voskuil, M. I., Visconti, K. C. et al. (2004). "*Mycobacterium tuberculosis* gene expression during adaptation to stationary phase and low-oxygen dormancy." Tuberculosis **84**(3–4):218-227.

Voss, M., Nimtz, M. et al. (2011). "Elucidation of the Dual Role of Mycobacterial MoeZR in Molybdenum Cofactor Biosynthesis and Cysteine Biosynthesis." PLOS ONE **6**(11):e28170.

Vynnycky, E. & Fine, P. E. (2000). "Lifetime risks, incubation period, and serial interval of tuberculosis." American Journal of Epidemiology **152**(3):247-263

Yu, Z., Lansdon, E. B. et al. (2007). "Crystal Structure of the Bifunctional ATP Sulfurylase – APS kinase from the Chemolithotrophic Thermophile *Aquifex aeolicus*." Journal of Molecular Biology **365**(3):732-743.

Zhao, C., Moriga, Y. et al. (2006). "On the interaction site of serine acetyltransferase in the cysteine synthase complex from *Escherichia coli*." Biochemical and Biophysical Research Communications **341**(4):911-916.

Zuniga, E. S., Early, J. et al. (2015). "The future for early-stage tuberculosis drug discovery." Future microbiology **10**(2):217-229.

Ågren, D., Schnell, R. et al. (2008). "Cysteine Synthase (CysM) of *Mycobacterium tuberculosis* Is an O-Phosphoserine Sulfhydrylase: Evidence for an alternative cysteine biosynthesis pathway in Mycobacteria." Journal of Biological Chemistry **283**(46):31567-31574.

Ågren, D., Schnell, R. et al. (2009). "The C-terminal of CysM from *Mycobacterium tuberculosis* protects the aminoacrylate intermediate and is involved in sulfur donor selectivity." FEBS letters **583**(2):330-336.